34323

National Library of Canada | Bibliothèque nationale du Canada

CANADIAN THESES ON MICROFICHE | *THÈSES CANADIENNES SUR MICROFICHE*

NAME OF AUTHOR/*NOM DE L'AUTEUR* RÉAL D'AMOURS

TITLE OF THESIS/*TITRE DE LA THÈSE* A NUMERICAL MODEL FOR HAILSTONE ICING

UNIVERSITY/*UNIVERSITÉ* UNIVERSITY OF ALBERTA

DEGREE FOR WHICH THESIS WAS PRESENTED/ *GRADE POUR LEQUEL CETTE THÈSE FUT PRÉSENTÉE* M. Sc.

YEAR THIS DEGREE CONFERRED/*ANNÉE D'OBTENTION DE CE GRADE* 1977

NAME OF SUPERVISOR/*NOM DU DIRECTEUR DE THÈSE* Dr. E. P. Lozowski

Permission is hereby granted to the NATIONAL LIBRARY OF CANADA to microfilm this thesis and to lend or sell copies of the film.

The author reserves other publication rights, and neither the thesis nor extensive extracts from it may be printed or otherwise reproduced without the author's written permission.

*L'autorisation est, par la présente, accordée à la BIBLIOTHÈQUE NATIONALE DU CANADA de microfilmer cette thèse et de prêter ou de vendre des exemplaires du film.*

*L'auteur se réserve les autres droits de publication; ni la thèse ni de longs extraits de celle-ci ne doivent être imprimés ou autrement reproduits sans l'autorisation écrite de l'auteur.*

DATED/*DATÉ* July 18 1977 SIGNED/*SIGNÉ* Réal D'Amours

PERMANENT ADDRESS/*RÉSIDENCE FIXÉ* 107- 282 Brookside Terrace
Edmonton Alberta

NL-91 (3-74)

National Library of Canada

Cataloguing Branch
Canadian Theses Division

Ottawa, Canada
K1A 0N4

Bibliothèque nationale du Canada

Direction du catalogage
Division des thèses canadiennes

## NOTICE

The quality of this microfiche is heavily dependent upon the quality of the original thesis submitted for microfilming. Every effort has been made to ensure the highest quality of reproduction possible.

If pages are missing, contact the university which granted the degree.

Some pages may have indistinct print especially if the original pages were typed with a poor typewriter ribbon or if the university sent us a poor photocopy.

Previously copyrighted materials (journal articles, published tests, etc.) are not filmed.

Reproduction in full or in part of this film is governed by the Canadian Copyright Act, R.S.C. 1970, c. C-30. Please read the authorization forms which accompany this thesis.

THIS DISSERTATION
HAS BEEN MICROFILMED
EXACTLY AS RECEIVED

## AVIS

La qualité de cette microfiche dépend grandement de la qualité de la thèse soumise au microfilmage. Nous avons tout fait pour assurer une qualité supérieure de reproduction.

S'il manque des pages, veuillez communiquer avec l'université qui a conféré le grade.

La qualité d'impression de certaines pages peut laisser à désirer, surtout si les pages originales ont été dactylographiées à l'aide d'un ruban usé ou si l'université nous a fait parvenir une photocopie de mauvaise qualité.

Les documents qui font déjà l'objet d'un droit d'auteur (articles de revue, examens publiés, etc.) ne sont pas microfilmés.

La reproduction, même partielle, de ce microfilm est soumise à la Loi canadienne sur le droit d'auteur, SRC 1970, c. C-30. Veuillez prendre connaissance des formules d'autorisation qui accompagnent cette thèse.

LA THÈSE A ÉTÉ
MICROFILMÉE TELLE QUE
NOUS L'AVONS REÇUE

NL-339 (3/77)

THE UNIVERSITY OF ALBERTA

# A NUMERICAL MODEL FOR HEAT TRANSFERS DURING HAILSTONE ICING

by

© RÉAL D'AMOURS

A THESIS

SUBMITTED TO THE FACULTY OF GRADUATE STUDIES AND RESEARCH

IN PARTIAL FULFILMENT OF THE REQUIREMENTS FOR THE DEGREE

OF MASTER OF SCIENCE

IN

METEOROLOGY

DEPARTMENT OF GEOGRAPHY

EDMONTON, ALBERTA

FALL, 1977

THE UNIVERSITY OF ALBERTA

FACULTY OF GRADUATE STUDIES AND RESEARCH

The undersigned certify that they have read, and recommend to the Faculty of Graduate Studies and Research, for acceptance, a thesis entitled "A Numerical Model for Heat Transfers during Hailstone Icing", submitted by Réal D'Amours in partial fulfilment of the requirements for the degree of Master of Science in Meteorology.

Edward Rozowski
.....
Supervisor

.....

.....

Date June 28 1977

DEDICATION

A Ginette

## ABSTRACT

A new spherically symmetric numerical model for hailstone icing has been devised which simulates certain aspects of the discrete nature of the accretion process, and which considers the heat transfers, including internal conduction, to be time-dependent. As a first approximation, a uniform layer of given thickness is accreted instantaneously over the entire surface of a spherical hailstone with initially homogeneous properties. The subsequent history of the deposit before the accretion of the next layer is divided into two stages. During the freezing stage, the deposit warms to $0^{\circ}C$ owing to the formation of ice dendrites and it exchanges heat with the environment and the interior of the stone while the remainder of the supercooled water freezes. If the entire deposit is frozen before the accretion of the next layer, it enters the cooling stage, where exchanges of heat with the environment and the interior give rise to a changing deposit temperature. During both of these stages, the interior temperature profile of the hailstone is also calculated as a function of time. By making the hypothesis that the individual droplets accreted on the hailstone would have a temperature cycle identical to that of a uniform deposit, a simple estimate of the temperature distribution over the hailstone surface is obtained. From such a distribution, the mean surface temperature, the standard deviation and the proportion of the stone surface in wet growth are calculated.

## ACKNOWLEDGEMENTS

I wish to express my sincere gratitude to Dr. Edward P. Lozowski for suggesting the topic of this thesis and for his continuing guidance and encouragement throughout the course of my studies. I specially want to thank Dr. Lozowski for giving me the exciting opportunity to attend the International Conference on Cloud Physics in Boulder, Colorado during the summer of 1976, as well as making possible my participation to the Eleventh Annual Congress of the Canadian Meteorological Society in Winnipeg.

Thanks are also due to Dr. R. B. Charlton and Dr. R. Gilpin for serving on my examining committee and to Dr. G. G. Goyer for his useful discussions and suggestions in the early stages of this research.

I would like to express my appreciation to Laura Smith for her kind and expert assistance in typing the final draft of this thesis.

This study and all other work required for the degree of Master of Science in Meteorology were conducted while on Educational Leave from the Atmospheric Environment Service of Canada.

TABLE OF CONTENTS


| | | Page |
|---|---|---|
| DEDICATION | | iv |
| ABSTRACT | | v |
| ACKNOWLEDGEMENTS | | vi |
| TABLE OF CONTENTS | | vii |
| LIST OF TABLES | | ix |
| LIST OF FIGURES | | xi |
| INTRODUCTION | | xiii |
| CHAPTER | | |
| 1 | EXISTING MODELS | 1 |
| | 1.1 An Early Model | 1 |
| | 1.2 Present Models | 3 |
| | 1.3 A Discrete Model | 8 |
| | 1.4 Other Work with Internal Conduction | 15 |
| 2 | A NEW MODEL | 16 |
| | 2.1 The Proposed Model | 16 |
| | 2.2 The Accretion Cycle | 19 |
| | 2.3 Heat Transfers | 21 |
| | 2.4 Other Heat Transfers | 25 |
| 3 | MATHEMATICAL METHODS | 29 |
| | 3.1 Two Initial Boundary Value Problems | 29 |
| | 3.2 Finite Differences and Grid Mesh | 35 |

| CHAPTER | | | Page |
|---|---|---|---|
| | 3.3 | The Crank-Nicholson Method . . . . . | 37 |
| | 3.4 | An Iterative Boundary Condition . . . . . | 39 |
| | 3.5 | Stability with Respect to Heat Transfer . . | 42 |
| 4 | A FEW PROGRAMMING CONSIDERATIONS . . . . . | | 47 |
| | 4.1 | Brief Description of Program . . . . . | 47 |
| | 4.2 | Re-initialization After One Cycle . . . . . | 48 |
| | 4.3 | Ice Fraction . . . . . | 50 |
| | 4.4 | Heat Content . . . . . | 51 |
| | 4.5 | Saturation Vapor Pressure . . . . . | 52 |
| | 4.6 | Thermodynamic Constants . . . . . | 53 |
| 5 | RESULTS AND DISCUSSION . . . . . | | 55 |
| | 5.1 | General Description . . . . . | 55 |
| | 5.2 | A More Representative Temperature . . . . . | 62 |
| | 5.3 | The Mechanism of Equilibrium . . . . . | 68 |
| | 5.4 | An Hypothesis . . . . . | 73 |
| | 5.5 | Effect of Deposit Thickness . . . . . | 78 |
| | 5.6 | Freezing Times . . . . . | 89 |
| 6 | SUMMARY AND CONCLUSIONS . . . . . | | 92 |
| BIBLIOGRAPHY . . . . . | | | 95 |
| APPENDIX 1. | Listing of Program . . . . . | | 98 |
| APPENDIX 2. | Listogram . . . . . | | 109 |

LIST OF TABLES


| Table | | Page |
|---|---|---|
| 1.1 | $\tau$ time necessary to freeze the deposit and for the hailstone to return to the initial heat content, compared to the time between the arrival of two successive layers, for two different thicknesses and different initial temperatures. | 14 |
| 2.1 | Heat transfers for a hailstone $5 \times 10^{-3}$ m in radius in the following cloud conditions: $T_a$ = 243K, P = 34.5 kPa, $w_f = 3.5 \times 10^{-3}$ kg $m^{-3}$. | 27 |
| 5.1 | Environmental conditions for the investigated growth segments. | 56 |
| 5.2 | Time necessary to accrete n layers of 25 μm for cloud conditions a, b, c, d, e and f. | 60 |
| 5.3 | Comparison of the final surface temperature $T_{sf}$ after the 20th accretion cycle with the equilibrium temperature $T_e$ for a 5.5 mm hailstone under different cloud conditions. | 61 |
| 5.4 | Average temperature ($^{o}$C) at different points along the hailstone radius, for the twentieth accretion cycle, under different cloud conditions. | 69 |
| 5.5 | Energy budgets of each accretion cycle for cloud condition a. | 71 |
| 5.6 | Net hailstone warming in Joules, for one accretion after a selected number of accretions. | 74 |
| 5.7 | Time averaged surface temperature over one accretion cycle, at selected hailstone sizes, for different deposit thicknesses, under cloud conditions a and b. | 80 |
| 5.8 | Final surface temperatures after one accretion cycle at selected hailstone sizes, for different deposit thicknesses $\delta R$, under cloud conditions a and b. | 81 |

| Table | | Page |
|---|---|---|
| 5.9 | Comparison of accretion cycles for cloud condition a, starting with a 4.5 mm radius hailstone at -11°C, adding (i) two 50 μm layers; (ii) four 25 μm layers. | 83 |
| 5.10 | Droplet radius required to form a 25 μm surface deposit, for different mean surface temperatures. | 88 |
| 5.11 | Standard deviation of the surface temperature distribution for different cloud droplets radii before accretion (calculated using Macklin's method). | 88 |
| 5.12 | Ratio of the estimated initial freezing time $t_i$ to the subsequent freezing time $t_f$ for different cloud conditions and mean surface equilibrium temperatures $T_e$. | 90 |

## LIST OF FIGURES


| Figure | | Page |
|---|---|---|
| 1.1 | Linear crystallization velocities (LCV) as a function of supercooling, after Hobbs (1974). | 9 |
| 4.1 | Problem of grid re-initialization when $\delta R$ the deposit thickness is larger than $\Delta r$ the grid point spacing. | 49 |
| 5.1 | Final surface temperature of the hailstone after N accretions for different cloud conditions: a, b, c, d, e (see Table (5.1)). | 57 |
| 5.2 | Ice fraction of surface deposit after N accretions of 25 μm layers, for cloud conditions f. | 59 |
| 5.3 | Internal temperature profiles for the first accretion cycle, after the freezing phase (those converging to $0^{\circ}C$) and after the cooling phase for cloud conditions a, b, c, d, e. | 63 |
| 5.4 | Internal temperature profiles for the twentieth accretion cycle, after the freezing phase and after the cooling phase. | 64 |
| 5.5 | Surface temperature as a function of time, during accretion number 20 for cloud conditions a, b, c, d, e. | 66 |
| 5.6 | Time averaged temperature profiles during the first accretion, for all of the dry growth conditions. | 67 |
| 5.7 | Standard deviation of the surface temperature distribution as a function of the mean temperature of the hailstone surface for a 5 mm radius hailstone. | 77 |

| Figure | | Page |
|---|---|---|
| 5.8 | Fraction of the surface in the wet growth regime as a function of the mean surface temperature. | 79 |
| 5.9 | Hailstone temperature profiles during a 50 μm growth. | 84 |
| 5.10 | Standard deviation of the surface temperature distribution as a function of deposit thickness (or droplet thickness after accretion) for cloud conditions a (upper curve) and b (lower curve). | 86 |
| A-1 | Listogram | 111 |

# INTRODUCTION

Hail formation can be studied through the analysis of hailstones. However, in order to explain the very complex structure (both inside and at the surface) of hailstones, hypotheses and assumptions have to be made about the microphysical processes taking place during their initiation and growth inside thunderclouds. These assumptions and hypotheses lead to the formulation of conceptual models.

Several microphysical models have been proposed (Schumann, 1938; Ludlam, 1950; List, 1963) to simulate heat transfers during hailstone growth. These were able to explain some of the observed features of hailstone structure such as opaque ice, clear ice or spongy ice. The purpose of this work is to review these studies and to present an improved numerical model which simulates more realistically some aspects of hailstone icing.

# CHAPTER 1

# EXISTING MODELS

## 1.1 An Early Model

Schumann (1938) was the first one to recognize that the surface temperature of an ice deposit formed by the accretion of supercooled water droplets should be warmer than the environment. He was also the first to consider that the latent heat of fusion released on freezing of the supercooled water had to be disposed of in one way or another. An energy budget was then established in which the latent heat released was transferred to the ambient air through conduction and convection and through evaporation of some of the water on the hailstone surface (sublimation of ice is not considered). In doing so the amount of heat conducted into the hailstone was neglected. By setting up a balance equation for heat transfers, which depended on the hailstone surface temperature, the cloud water content, the air temperature and the pressure, he was able to solve for an equilibrium surface temperature. Interestingly, his result indicated no dependence of the equilibrium temperature on the hailstone dimensions. So for a given cloud model, the hailstone temperature would be a function of height alone. This peculiarity is basically

due to an erroneous formulation of the ventilation coefficients used in expressing the heat and water vapour transfers.

The basic assumptions of Schumann's model are that the hailstone is a perfectly smooth sphere, and that it collects all the cloud water (but no ice particles) encountered in its path. Using results published by Bilham and Relf (1937), the terminal velocity of the stone is calculated to obtain the rate of accretion of supercooled water and therefore the rate at which latent heat is released, assuming total freezing. This should be equal to the rate at which the heat is dissipated through conduction to the air and through evaporation of water. In order to calculate the dissipative terms, Schumann postulates the existence of a "stagnant layer of air" around the falling hailstone inside of which all transports are due to molecular processes. According to his calculations the rate of heat dissipation per unit area has the same dependence on the radius as the terminal velocity so that this variable drops out of the balance equation.

Another important concept which this model gave rise to is the concept of critical liquid water content. Schumann was the first one to realize that there was a limit to the amount of supercooled water which could be frozen on the hailstone surface. Above that amount the rate of dissipation would be insufficient to balance the rate of production of latent heat. The hailstone would then warm up to $0^{o}C$ and the excess collected water would not freeze. This limit is referred to as the critical liquid water content. Schumann thought that the excess collected water would be thrown off in the form of droplets. Again the value of the critical liquid water content

shows no dependence on the hailstone dimensions and is a function only of the cloud parameters.

Although this model leads to erroneous conclusions, it was a first attempt to simulate realistically the heat transfers and it had the merit of leading to the very important concept of critical liquid water content.

## 1.2 Present Models

Using more accurate measurements of the drag and ventilation coefficients obtained with the aid of wind tunnels, Ludlam (1950, 1951, 1958) corrected the heat balance equation set up earlier by Schumann. Essentially the same equation was used except for improved formulations of the heat transfers due to convection and conduction and due to evaporation. This results in an equilibrium temperature which is a function of the hailstone size, as well as of the external cloud conditions. The critical liquid water content above which all the collected supercooled water cannot be frozen on the hailstone surface is also derived from this model, and it has a dependence on the hailstone radius. When a hailstone enters a region for which the liquid water content exceeds the critical value, it enters a growth regime which Ludlam describes as the wet growth regime. In these conditions a film of liquid water covers the hailstone surface. Ludlam believed that most of this water would be shed by the hailstone. During this stage clear ice forms. Opaque ice occurs during the dry growth regime, where the cloud water content is subcritical and the accreted water freezes completely. The alternating layers of clear and opaque ice

characteristic of large hailstones are then explained by "... successive passages through critical conditions caused by changes in radius, falling speed, temperature, pressure and liquid water content in the cloud." (Ludlam, 1950).

This type of continuous model was given in its most complete form by List et al. (1963, 1965, 1967). The basic assumption of the model which is also an implied assumption of the earlier models, is the quasi steady-state assumption. It is supposed that the rate of change of the hailstone radius is sufficiently slow that the heat transfer rates vary only very slowly and the hailstone remains at the equilibrium temperature. Again the heat transferred to the hailstone itself is assumed to be negligible. Calculations are done for spherical hailstones, although later extended to spheroidal hailstones (1967).

Under these assumptions, the general heat balance equation is set up as follows:

$$Q_{CC} + Q_{ES} + Q_{CP} + Q_F = 0 \qquad (1.1)$$

where $Q_{CC}$ is the rate of heat exchange by conduction and convection; $Q_{ES}$ is the rate of heat exchange due to evaporation or sublimation; $Q_{CP}$ is the rate of heating of the accreted cloud droplets (in order for them to rise to the surface temperature); and $Q_F$ is the rate of release of latent heat by the freezing of the supercooled water droplets.

The originality of this model, besides the thoroughness in the expression of each term of the balance equation, is that it allows for incomplete freezing of the deposit. It is now known that spongy ice (a mixture of ice and water) could play an important role in the formation of hailstones. This model, assuming that none or only part of the non-frozen water is shed by the hailstone, permits one to make some conclusion about the conditions of formation of this particular type of ice.

Upon writing each term as a function of the surface temperature and of the ice fraction of the deposit, the balance equation can be rewritten as:

$$\frac{1.68k(t_d - t_a) + c_{1,2}\, D_{wa}\, T_a^{-1}(e_{SH} - e_{SV})}{.785\,(L_f I - \bar{c}_w (t_d - t_a))} = \nu^{\frac{1}{2}} v^{\frac{1}{2}} D^{\frac{1}{3}} E \theta^{-1} w_f \,. \qquad (1.2)$$

$k$: thermal conductivity of the air (cal $cm^{-1}$ $^oC^{-1}$)

$t_d$: deposit equilibrium temperature ($^oC$)

$t_a$: air temperature ($^oC$)

$c_{1,2}$: constant which contains the product of mass transfer coefficient for water vapour and latent heat of vaporization or sublimation. It takes the value .207 cal $^oC$ $cm^{-3}$ $mb^{-1}$ for liquid-gas transitions and .235 cal $^oC$ $cm^{-3}$ $mb^{-1}$ for solid-gas transitions.

$D_{wa}$: diffusivity of water vapor in air ($cm^2$ $s^{-1}$)

$T_a$: absolute temperature of the air (K)

$e_{SH}$, $e_{SV}$: saturation vapor pressure over the hailstone surface and for the environment

$\nu$: kinematic viscosity ($cm^2\ s^{-1}$)

D: diameter of spherical hailstone (cm)

$\theta$: roughness factor

E: collection efficiency

$w_f$: cloud water content ($g\ cm^{-3}$)

$L_f$: latent heat of fusion of water ($cal\ g^{-1}$)

$\bar{c}_w$: specific heat capacity averaged from $t_a$ to $t_d$ ($cal\ g^{-1}$)

I: ice fraction of deposit

For given cloud conditions, equation (1.2) relates D, I, $t_d$: respectively, the hailstone diameter, the ice fraction, and the temperature of the deposit. Ignoring the finite freezing time of the deposit, $I < 1$ only if $t_d = 0^oC$. Therefore for a given hailstone diameter and given cloud conditions, the temperature and the ice fraction (assuming no water is shed) are uniquely determined. Calculations were done for a "typical" cloud model relating air temperature, pressure and height. The results are presented in graphical form in the well-known "Listograms" (see Appendix 2).

This model was also extended by List et al. (1967) to include melting. In that case the warmer environment would be giving heat to the stone, through conduction and convection, while condensation of water vapor on the colder hailstone surface would release latent heat of vaporization; this heat would then be used

to melt some of the ice on the hailstone.

As mentioned earlier, the basic assumption of the models presented above is the quasi steady-state assumption. However, when a hailstone grows, its terminal velocity increases, which in turn increases its rate of accretion. Since the rate of accretion, and, therefore, the rate of latent heat release, increases faster than the dissipating terms, the surface temperature increases with time. According to the steady state models, this change in temperature should be sufficiently slow to be of no real significance. Nevertheless, the effects of a rising surface temperature were investigated by Pellet and Dennis (1974) using a modified version of the continuous model. In this model heat transfers with the underlying hailstone are allowed. Writing the balance equation for this model, we have

$$Q_i = \frac{d}{dt}(M_i C_i T_s) = Q_{CC} + Q_{ESC} + Q_{CP} + Q_F , \qquad (1.3)$$

where $M_i$, $C_i$, $T_s$ are, respectively, the mass, specific heat capacity, and absolute temperature of the hailstone. Calculations were done for a hailstone growing in a stationary one-dimensional cloud model. Comparing the results with those obtained when $Q_i = 0$, as in the steady-state models, it is found that there is very little difference between the two and that the stone adjusts fairly quickly to the equilibrium temperature. However, this last model assumes that the hailstone has a uniform temperature, and that the heat is conducted instantaneously into the stone interior,

which implies an infinite thermal conductivity.

## 1.3 A Discrete Model

The underlying assumption of all the models described above is that the accretion of supercooled water is continuous (whence the label continuous model). They treat the cloud water as if it were a gas whose density is the liquid water content. In reality the accretion process is discontinuous with the water being accreted in lumps as the individual droplets impinge on the hailstone surface.

Macklin and Payne (1967) made a theoretical investigation of ice accretion emphasizing the freezing of the individual droplets. Once a supercooled water droplet impinges on the surface of a hailstone, the equilibrium is disturbed and ice is nucleated. How rapidly and in which manner the ice phase will develop inside the droplet is not clear. It should depend greatly on the molecular mechanisms involved in the solidification process; but it should also depend on the rate at which the latent heat of fusion can be dissipated to the surroundings. Several authors (Macklin and Ryan, 1965) have investigated the growth of ice in bulk supercooled water at strong supercooling; in this case, because of the heat limitations, the growth takes a dendritic form. In the case of lower supercoolings (less than $2.5^{o}C$), the growth rate is slower and more orderly. Estimates of growth velocities of ice dendrites in supercooled water as a function of total supercooling are given in Figure 1.1.

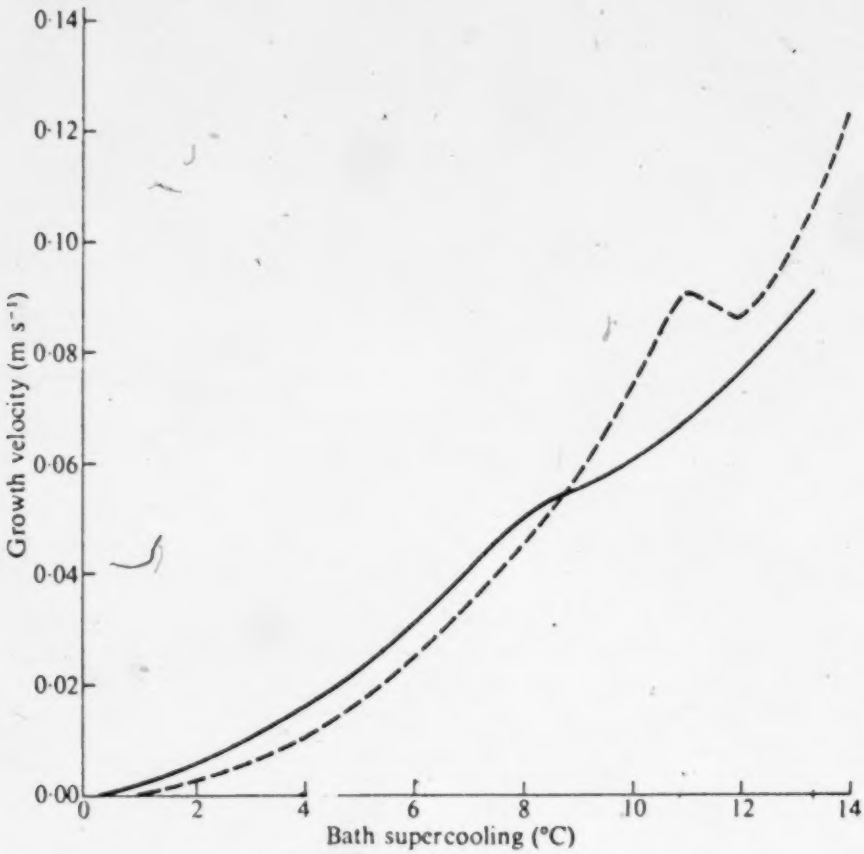


Figure 1.1 Linear crystallization velocities (LCV) as a function of supercooling, after Hobbs (1974). LCV are obtained by measuring the growth of ice in supercooled water contained in narrow tubes. The continuous line represents data obtained by Tammann and Büchner and the dashed line, data from Pruppacher.

We are not aware of measurements of the growth rate of ice inside supercooled cloud droplets, but on the basis of Figure 1.1 one can expect that the initial growth should be very rapid. In order to study the freezing process in the dry growth regime of a hailstone, Macklin and Payne formulated the following model.

> "A newly arrived droplet (on the hailstone surface) is nucleated and its temperature rises rapidly towards $0^{o}C$.... This will be called the initial freezing. ... The subsequent freezing rate is controlled partly by heat conduction into the deposit and partly by forced convection and evaporation to the environment. When the freezing process is complete the droplet begins to cool by forced convection and in a steady state it cools until, on the average, the initial mean temperature of the deposit is regained before the arrival of the next droplet when the procedure is repeated. We distinguish therefore three main phases, involving different physical processes, during which the heat of a droplet is removed: the initial freezing, the subsequent freezing and the cooling phase. Although there is some overlapping of these three phases, the total time, $\tau$, it takes to remove the heat liberated by the droplet may be conveniently regarded as the sum of three individual times, namely,
>
> $$\tau = t_i + t_f + t_c . \qquad (1.4)$$
>
> In the steady state situation $\tau$ is then the average interval of time between the arrival of successive droplets."

(Macklin and Payne, 1967, p. 201-202).

In order to simplify the calculations, the authors consider the freezing of a uniform layer of supercooled water of thickness $\delta R$ on a sphere of radius R, initially at a uniform temperature $T_d$ so that heat flows will be in the radial direction only. Right at the outset it is assumed that $t_i$ is negligible with respect to $t_f$ (although it is found later that this is not quite true for very thin

layers, less than 1 μm) and that no heat is exchanged outside the deposit during that time. So in practice, the process starts with an ice-water deposit initially at $0^{o}C$, and during the subsequent freezing, heat is conducted inside the sphere, and heat is transferred to the air by forced convection and evaporation. The deposit is said to be frozen when all the latent heat available has been expended. Therefore,

$$Ht_f + q_f = \rho_w \delta R \left\{ L_f + c_w (T_a - T_m) \right\} \qquad (1.5)$$

The L.H.S. of equation (1.5) is the sum of the heat given to the environment at the rate H during time $t_f$ and $q_f$ is the heat conducted inside the hailstone. The R.H.S. of equation (1.5) is the latent heat available after warming the accreted deposit to the melting point $T_m$. Macklin and Payne assumed without much evidence that $Ht_f$ is small enough to be negligible with respect to $q_f$; also, in the evaluation of $q_f$, they neglected the spherical effects by using the solution for linear heat flow into a semi-infinite body having a plane surface. We will see later that this last assumption is not fully justified. Nevertheless, with the aid of these assumptions, Macklin and Payne obtain the following expression for the (subsequent) freezing time:

$$t_f = \frac{\pi \rho_w^2 \delta R^2 \left\{ L_f + c_w (T_a - T_m) \right\}^2}{4 \rho_i c_i V^2 K} , \qquad (1.6)$$

where $\rho_w$ is the density of water, $\delta R$ the deposit thickness, $L_f$ the

latent heat of fusion for water, $c_w$ the specific heat capacity for water (although $L_f$ and $c_w$ are temperature dependent, this is not considered by the authors), V is the absolute value of $T_d$ expressed in Celsius, and $\rho_i$, $c_i$, K are, respectively, the density, the specific heat capacity and the thermal conductivity for ice; $T_a$ and $T_m$ are the air temperature and the melting temperature.

Next comes the cooling phase. The authors' ideas about this stage are somewhat confusing. It seems as if they assume that the final deposit (hailstone) temperature $T_d$ is determined by external conditions (and can be obtained by equations similar to those of the List model) and that the duration of the cooling phase $t_c$ must be just what is needed for the deposit to return to $T_d$; the arrival of the next layer must then await the completion of this phase and the achievement of $T_d$. In other words, the authors are investigating the processes by which a mean equilibrium deposit temperature is achieved, and they do not question this deposit temperature itself. The hypothesis is: In order to return the sphere to its initial state (i.e., where the average temperature is $T_d$), the heat conducted into the sphere during the freezing process together with that given out by the ice layer in cooling from $T_m$ to $T_d$ have to be removed. Thus the heat per unit area to be removed is

$$q_c = q_f + \rho_w \delta R c_i (T_m - T_d). \qquad (1.7)$$

The rate at which heat is dissipated to the environment depends on the difference between the surface temperature of the sphere and that of the air, as well as on the difference between the saturated vapor

pressure over the hailstone and that in the environment. Even though the dependence of the vapor pressure on the temperature is far from linear, the authors assume linearity, in order to be able to use the solution of the heat equation with the radiation boundary condition. No justification is given to support this assumption; it seems very difficult to evaluate the type of error introduced by this procedure. (Further discussion of this procedure is given in section 3.1.)

Interestingly, results show that in order to remove all the heat absorbed during the freezing phase, the surface temperature falls below the original temperature $T_d$. Furthermore, it is found that this heat is dissipated some time before the arrival of the next layer so that the hailstone becomes somewhat colder than initially. Table 1.1 gives a comparison of the time necessary to freeze the deposit and for the hailstone to return to the initial heat content, and the time between the arrival of two successive layers. It is seen that the difference is quite significant especially for thick layers at cold conditions. This could mean that large cloud droplets could form deposits that are colder than those resulting from an equivalent number of smaller droplets. Although these findings were acknowledged by Macklin and Payne, no discussions of the reasons or the possible implications are presented.

Table 1.1

$\tau$ time necessary to freeze the deposit and for the hailstone to return to the initial heat content, compared to the time between the arrival of two successive layers, for two different thicknesses and different initial temperatures. $\tau$ is the sum of $t_f$ and $t_c$ as calculated by Macklin and Payne (1967, Table 6). $\Delta t$ is the time necessary for the hailstone to grow by the given thicknesses, using Ludlam's (1958, p. 49) formula. $T_d$ is the initial temperature of the hailstone (1.5 cm in diameter) and the values correspond to the equilibrium temperature calculated for the -20°C level of the Wokingham storm (Browning and Ludlam, 1962) for liquid water contents also given by Macklin and Payne (1967, Table 6).

| | 1 μm | | | 15 μm | |
|---|---|---|---|---|---|
| $T_d$(°C) | $\tau$(s) | $\Delta t$(s) | $T_d$(°C) | $\tau$(s) | $\Delta t$(s) |
| -2 | $7.12 \times 10^{-2}$ | $7.16 \times 10^{-2}$ | -2 | 1.05 | 1.08 |
| -5 | $9.51 \times 10^{-2}$ | $9.57 \times 10^{-2}$ | -5 | 1.38 | 1.42 |
| -10 | $1.70 \times 10^{-1}$ | $1.72 \times 10^{-2}$ | -10 | 2.46 | 2.56 |

## 1.4 Other Work with Internal Conduction

The effects of internal conduction were also investigated by Hitschfeld and Stauder (1967). They calculated the temperature change of a hailstone falling in clear air and found that there was a considerable lag accompanied by a significant internal temperature gradient (2-3°C from surface to center). For a hailstone falling through supercooled rain, they found that the effects of internal conduction were over-shadowed by the latent heat effect of supercooled water.

Goyer et al. (1969) used the heat diffusion equation to calculate the rate of freezing of spongy hail. Their theoretical calculations were compared with experimental measurements showing very good agreement between the two. Applying their numerical model to a simplified thunderstorm model, they concluded that it is unlikely that sufficient time is available for large, spongy hailstones to freeze completely.

# CHAPTER 2

# A NEW MODEL

## 2.1 The Proposed Model

All the continuous models described in Chapter 1 neglected the effects of a finite thermal conductivity for the hailstone. Macklin's results indicated the possibility of significant differences when the discrete nature of the accretion process was taken into account; however, only one accretion cycle was examined and the approximations made were not totally satisfactory. For these reasons, it was decided to develop a model which would further investigate the discrete nature of the freezing process by studying the freezing and cooling cycles of several accreted layers with the proper heat transfers. This model would also look into the effects of allowing heat conduction within the hailstone due to internal temperature gradients.

The proposed model is basically an extension of the model developed by Macklin and Payne, and described in the first chapter. The two major differences are that the accretion cycle is repeated successively several times, with the temperature profile resulting from the previous cycle being the initial condition for the next one. Also, the heat conduction equation, together with the boundary conditions

is solved by means of numerical methods, thereby eliminating the necessity of making approximations to the analytic solutions in order to make them readily solvable.

The main assumptions of the model are spherical symmetry (spherical hailstone), and constant density and thermal conductivity throughout the hailstone interior. It is also assumed that the deposit has the same properties as the hailstone, and that it is accreted uniformly over the surface. Because of these assumptions the mathematical problem is spherically symmetric: the temperature and ice fraction are functions of the radius and time and we are concerned with radial heat transfers only.

The model considers a spherical hailstone growing under constant cloud conditions. Melting and refreezing are not investigated; however, the case of incomplete freezing in the wet growth regime is taken into account.

Under the continuous growth hypothesis, the time necessary for a spherical hailstone to grow by the radial increment $\delta R$ is given by (Ludlam, 1958)

$$\tau = \frac{4\rho_i}{v_t E w_f} \delta R \ , \qquad (2.1)$$

where $v_t$ is the terminal velocity of the stone, $w_f$ the liquid water content, E the collection efficiency, $\rho_i$ the density of the deposit. In our model it is assumed that a deposit of thickness $\delta R$ is instantaneously accreted; therefore, $\tau$ is taken to be the mean time between the arrival of each layer, or the time duration of one cycle; alternatively this could be interpreted to be the mean time between

the arrival of two droplets over the same area on the hailstone surface.

The choice of $\rho_i$, the density of ice, for the deposit density is justified by the fact we are assuming the deposit to have the same properties as the hailstone. It is not at all clear what should be the density of a hailstone since it could vary greatly, depending on the surface temperature at the time of accretion (Macklin, 1962). At any rate, the value of 917 kg $m^{-3}$ was selected, as suggested by List (1963), although values as low as 300 kg $m^{-3}$ have been measured for rime ice formed on cylinders under very cold conditions (Macklin, 1967).

For a hailstone, the collection efficiency can be set equal to unity (Ludlam, 1958; List, 1963). However this ignores possible water shedding at high liquid water contents in the wet growth regime (List et al., 1976). Substituting in equation (2.1) we get

$$\tau = 3{,}600 \frac{\delta R}{v_t \cdot w_f} \text{ (SI)}. \qquad (2.2)$$

When a hailstone is at the terminal velocity, the drag force exerted by the air is equal to the weight of the hailstone. For a falling sphere the terminal velocity is given by (List et al., 1967)

$$v_t = 1.15 \left[\frac{g\ \rho_i D}{\rho_a\ c_D}\right]^{\frac{1}{2}} \text{ (SI)}, \qquad (2.3)$$

where g is the acceleration due to gravity (set at 9.80 m $s^{-2}$), $\rho_i$ the

hailstone density, D the hailstone diameter, $\rho_a$ the air density, $c_D$ the drag coefficient. For hailstones of diameter larger than $5 \times 10^{-3}$ m, the drag coefficient is nearly constant and can be set equal to 0.50 (List et al., 1967). However, Strong (1974) suggested a value closer to 0.6.

Substituting in equation (2.2) we get

$$v_t = 1.16 \times 10^{+2} \left[\frac{RT}{p}\right]^{\frac{1}{2}} . \qquad (2.4)$$

Here, T is the air temperature in degrees Kelvin, R is the hailstone radius in m, and p is the pressure in kPa.

## 2.2 The Accretion Cycle

Within one cycle, three processes are taking place. First, the deposit is accreted instantaneously. It is assumed that dendrites are nucleated quasi-instantaneously and uniformly within the deposit so that a negligible amount of heat is exchanged outside the deposit. The validity of this assumption has been discussed by Macklin (1967) and was analyzed in the first chapter. Therefore, all the latent heat released at that stage is used up in warming the deposit to $0^{o}C$. Once the deposit has reached the melting temperature, no more freezing is possible without some mechanism for dissipating the released latent heat and the resulting ice fraction is given by

$$I = \frac{\bar{c}_w |t_a|}{L_f(t_a) + (\bar{c}_w - \bar{c}_i)\ |t_a|} \qquad (2.5)$$

where $t_a$ is the air temperature, $\bar{c}_w$ and $\bar{c}_i$ are respectively the water and the ice specific heat capacity averaged from $t_a$ to $0^oC$. This formula supposes that the latent heat released on freezing of the fraction I of the supercooled water at the temperature $t_a$ is used up in warming the entire deposit, ice and water alike, to $0^oC$. It is equivalent to the following shorter expression

$$I = \frac{\bar{c}_w \, |t_a|}{L_f(0^oC)} \quad . \tag{2.6}$$

However the physical meaning here is not realistic. It seems in fact to imply that all the supercooled water warms to $0^oC$, and that the heat needed for this warming is provided by freezing a certain portion I of the deposit at $0^oC$ which is impossible. This initial instantaneous phase corresponds to the initial freezing stage of Macklin's model.

Next comes the freezing phase, analogous to Macklin's subsequent freezing. During this period, the remaining liquid water (or part of it) will be frozen. The total mass of unfrozen water is given by

$$M_r = 4\pi R^2 \delta R \rho_i \, (1 - I) \, , \tag{2.6}$$

and the total available latent heat is given by

$$H_{max} = L_f(0^oC) M_r = 4\pi R^2 \delta r \rho_i \, (1 - I) \, L_f(0^oC) \, . \tag{2.7}$$

Here again $\rho_i$ is used according to the initial assumption that the deposit has the same density as the hailstone. The deposit temperature is maintained at $0^{o}C$ as long as there is liquid water present: the available latent heat is disposed of by exchanges with the colder environment and with the hailstone interior. If all the deposit becomes frozen before the arrival of the next layer, that is, if all the latent heat available has been released, the hailstone enters the cooling phase. The name itself is quite explicit, meaning that the hailstone will transfer energy to the colder environment which then produces a lowering of the temperature.

During the next cycle, another layer of supercooled water is accreted, and the process is repeated, with the radial temperature profile resulting from the previous calculations as the initial condition.

## 2.3 Heat Transfers

When a hailstone grows in a thunderstorm cloud, energy is absorbed and released at its surface in several ways. As was discussed earlier, latent heat is released by the freezing of the accreted supercooled water droplets; heat is also absorbed in warming the accreted deposit, as well as the hailstone itself. Heat is dissipated by forced convection and conduction to the ambient air, and latent heat is absorbed by evaporation or sublimation of some of the deposit. There is also heat generation due to the absorption of the kinetic energy of the accreted deposit and due to friction between the moving hailstone and the environmental air. Finally, heat can be absorbed

or released by radiative transfers.

In our model the total heat of fusion available is given by equation (2.7)

$$H_{max} = L_f(0^oC)\ (1 - I)\ 4\pi R^2 \delta R \rho_i \ . \qquad (2.7)$$

The energy released by the freezing of the fraction I of the deposit has been used up in warming the latter to $0^oC$. The only other heat transfers to be considered in this model are the heat conducted to the hailstone interior, heat transfers due to conduction and forced convection to the environmental air, and the latent heat absorbed by evaporation or sublimation of part of the deposit. The remaining transfers are assumed to be negligible for reasons which we discuss in section 2.4.

The rates at which the hailstone loses heat because of conduction and forced convection, $Q_{CC}$, and because of evaporation or sublimation, $Q_{ES}$, are given by List (1963) and List et al. (1965, 1967),

$$Q_{CC} = 1.68\ k\theta\ Re^{\frac{1}{2}}\ D\ (t_d - t_a)\ , \qquad (2.8)$$

$$Q_{ES} = c_{1,2}\ \theta\ D_{wa}\ T_a^{-1}\ Re^{\frac{1}{2}}\ D\ (e_{SH} - e_{SV})\ . \qquad (2.9)$$

$\theta$ is the roughness factor which is defined as the relationship between the heat transfer through a natural (rough) surface and the heat transfer through a smooth surface; it is set at 1.5 (List, 1963). Re is the Reynolds number. For a sphere falling at the terminal velocity

in air it is given by

$$Re = \frac{v_t D}{\nu} \quad . \tag{2.10}$$

$v_t$ and D are respectively the terminal velocity and diameter of the sphere, and $\nu$ is the kinematic viscosity of the air. According to List et al. (1967), (p in kPa),

$$\nu = 5.54 \times 10^{-8} p^{-1} T_a^{1.8} \quad (m^2 \ sec^{-1}) \ ; \tag{2.11}$$

substituting in (2.8) together with equation (2.4) for $v_t$,

$$Re = 4.19 \times 10^{9} R^{1.5} T_a^{-1.3} p^{.5} \quad . \tag{2.12}$$

R is the radius of the sphere (m), $T_a$ the air temperature in K, and p the pressure in kPa.

k is the thermal conductivity of the air. According to the thermodynamic theory for dilute gases (Reif, 1965),

$$k \propto T^{\frac{1}{2}} \quad . \tag{2.14}$$

However, we find that the following formula approximates values of the thermal conductivity of the atmosphere, according to the American Institute of Physics Handbook (AIPH) 1972, up to the third decimal place in the temperature range of interest.

$$k = 1.549 \times 10^{-4} T^{.9} \ (W \ m^{-1} \ K^{-1}) \tag{2.15}$$

The diffusivity of water vapor in air is calculated according to AIPH data also by

$$D_{wa} = .219 \left(\frac{T_a}{273}\right)^{1.75} \left(\frac{1013.25}{p}\right) (cm^2\ s^{-1}) , \qquad (2.16)$$

although Hall and Pruppacher (1976) suggest

$$D_{wa} = .211 \left(\frac{T_a}{273}\right)^{1.94} \left(\frac{1013.25}{p}\right) (cm^2\ s^{-1}) . \qquad (2.17)$$

In both equations the pressure is in mb. In SI units equation (2.16) becomes (p in kPa)

$$D_{wa} = 1.21 \times 10^{-7}\ T_a^{1.75}\ p^{-1}\ (m^2\ s^{-1}) . \qquad (2.18)$$

$c_{1,2}$ is the product of several constants and the latent heat of sublimation or vaporization. It takes the value

$c = 9.84 \times 10^4\ J\ m^{-3}\ kPa^{-1}$ and $c_2 = 8.67 \times 10^4\ J\ m^{-3}\ kPa^{-1}$

when the air temperature is less than $-20^oC$ or at $0^oC$, respectively. Between $-20^oC$ and $0^oC$, $c_{1,2}$ varies linearly with temperature from $c_1$ to $c_2$ (List et al., 1967).

Upon substitution of all these constants in equations (2.8) and (2.9) we obtain

$$Q_{CC} = 50.5\ R^{1.75}\ (T \cdot p)^{.25}\ (t_d - t_a)\ \ (W) \qquad (2.19)$$

$$Q_{ES} = 2.35\ c_{1,2}\ T_a^{.1}\ p^{-.75}\ R^{1.75}\ (e_{SH} - e_{SV})\ \ (W) \qquad (2.20)$$

## 2.4 Other Heat Transfers

The drag force for a hailstone falling at its terminal velocity is equal to its weight, so that the heat generated by friction per unit time is given by

$$Q_{FR} = mgv_t \ , \tag{2.21}$$

where m is the hailstone mass and g the gravitational acceleration. For a hailstone of density $\rho_i = 900$ kg $m^{-3}$

$$Q_{FR} = 4.29 \times 10^5 \, R^{3.5} \left(\frac{T}{p}\right)^{.5} \ (W) \ . \tag{2.22}$$

If the kinetic energy of the accreted deposit was entirely transformed into heat, the heat generated during one accretion cycle would be

$$K.E. = 4\pi R^2 \rho_i \delta R \, \frac{v_t^2}{2} \ , \tag{2.23}$$

assuming that the cloud droplets have a negligible terminal velocity compared to that of the hailstone. Since the energy would be delivered during a time $\tau$, we can calculate an equivalent rate of release

$$Q_{KE} = 4\pi R^2 \rho_i \delta r \, \frac{v_t^2}{2} \, \frac{1}{\tau} \ . \tag{2.24}$$

In order to estimate the energy absorbed or released because of radiative transfers, we investigate the infrared and the visible parts separately. For the infrared, assuming that the hailstone and

the water vapor in the cloud are perfect blackbodies, the radiative flux out of the hailstone would be given by

$$Q_{IR} = 4\pi R^2 \sigma (T_H^4 - T_A^4) , \qquad (2.25)$$

where $\sigma$ is the Stefan-Boltzmann constant, $T_H$ and $T_A$ the hailstone and air temperatures. It has been estimated (Kuo-Nan Liou, 1976) that cumulonimbus clouds reflect 80-90 percent of the incident solar radiation. It seems, therefore, reasonable to assume that 10 percent of the solar constant would be an acceptable estimate for the diffuse visible light in the heart of a thunderstorm. Secondly, we assume that an average hailstone absorbs at most 10 percent of the visible light incident on its surface (Hobbs, 1974). Therefore, the net radiative flux from the hailstone would be

$$Q_R = 4\pi R^2 (\sigma (T_H^4 - T_A^4) - .01\ s) , \qquad (2.26)$$

where s is the solar constant $1.395 \times 10^3$ W $m^{-2}$.

In order to obtain an idea of the relative magnitude of all these heat transfers, calculations were made for a hailstone of radius $5.0 \times 10^{-3}$ m, in the following cloud conditions: $T_a$ = 243K, p = 34.5 kPa, $w_f = 3.5 \times 10^{-3}$ kg $m^{-3}$. The equilibrium temperature for these conditions according to the List et al. (1965) model would be about 262K. Results are shown in Table 2.1, according to these

$$\frac{Q_{FR} + Q_R + Q_{KE}}{Q_{CC} + Q_{ES}} = .004 . \qquad (2.27)$$

Table 2.1

Heat transfers for a hailstone $5 \times 10^{-3}$ m in radius in the following cloud conditions: $T_a = 243K$, $p = 34.5$ kPa, $w_f = 3.5 \times 10^{-3}$ kg $m^{-3}$. $Q_{CC}$ is the heat exchange due to conduction and convection to the surrounding air; $Q_{ES}$: heat exchange due to evaporation or sublimation; $Q_{FR}$: heat production due to friction; $Q_R$: radiation absorbed by the hailstone; $Q_{KE}$: heat production due to the transformation of the deposit kinetic energy.

| $Q_{CC}$ (W) | $Q_{ES}$ (W) | $Q_{FR}$ (W) | $Q_R$ (W) | $Q_{KE}$ (W) |
|---|---|---|---|---|
| .863 | .530 | .010 | -.017 | .002 |

Therefore under these conditions and probably under most other conditions encountered by a hailstone, it seems to be quite reasonable to neglect $Q_{FR}$, $Q_R$ and $Q_{KE}$ altogether.

# CHAPTER 3

## MATHEMATICAL METHODS

### 3.1 Two Initial Boundary Value Problems

The temperature change inside the hailstone is determined by the heat diffusion equation

$$\frac{\partial}{\partial t}(\rho_i c_i T) - \vec{\nabla}\cdot(K_i \vec{\nabla} T) - g = 0 \qquad (3.1)$$

where $\rho_i$ is the density of the hailstone, $c_i$ the specific heat capacity, T the absolute temperature, $K_i$ the thermal conductivity, and g the heat generated per unit volume. According to the assumptions made in Chapter 2, $\rho_i, c_i, K_i$ are constant in time and space, g is zero (freezing of spongy ice inside the hailstone is not considered since the external cloud conditions are kept constant), and we have radial symmetry; the equation therefore reduces to

$$\frac{\partial T}{\partial t} = k\left[\frac{\partial^2 T}{\partial r^2} + \frac{2}{r}\frac{\partial T}{\partial r}\right], \qquad (3.2)$$

where k, the thermal diffusivity is given by

$$k = \frac{K_i}{\rho_i c_i} \qquad (3.3)$$

For further simplification consider the following function $u = r(T - 273)$, where u is the product of the radial distance and the temperature in degrees Celsius. Upon substitution in equation (3.2) we have

$$\frac{\partial u}{\partial t} = k \frac{\partial^2 u}{\partial r^2} \tag{3.4}$$

with the boundary condition that $u = 0$ at $r = 0$.

In practice, the accretion cycle consists of two phases which form two distinct initial boundary value problems (IBVP). For the first phase, the surface temperature is maintained at $0^{o}C$ and the initial temperature profile $f(r)$ is given. The time duration of the phase, $t_f$, is not known but has to be determined from the problem. Stated formally this IBVP can be written as follows

$$\frac{\partial u}{\partial t} = k \frac{\partial^2 u}{\partial r^2}, \qquad 0 \leq r < R, \tag{3.4}$$

$$u(0,t) = u(R,t) = 0, \tag{3.5}$$

$$u(r,0) = f(r). \tag{3.6}$$

The solution to this problem is given by Carslaw and Jaeger (1959),

$$u(r,t) = \frac{2}{R} \sum_{n=1}^{\infty} \sin\left(\frac{n\pi r}{R}\right) \exp\left[\frac{-kn^2\pi t}{R^2}\right] \int_0^R f(\rho)\sin\left(\frac{n\pi\rho}{R}\right) d\rho. \tag{3.7}$$

Since the model considers only conditions where the air temperature is below freezing, in order for the hailstone surface temperature to be maintained at $0^{o}C$, heat must be generated at the surface. We assume that the thickness of the accreted deposit is sufficiently small relative to the radius of the sphere for the deposit to be considered coincident with the surface. The source of energy is then the latent heat of fusion released on freezing some of the liquid water trapped in the deposit. The maximum amount of heat available for this is given by equation (2.7). The heat fluxes from the hailstone to the air are given by equations (2.8) and (2.9)

$$Q_V(u(R,t)) = Q_{CC} + Q_{ES} , \tag{3.8}$$

and the heat flux from the hailstone surface to its interior is given by

$$Q_i = 4\pi R^2 K_i \left.\frac{\partial T}{\partial r}\right|_R = 4\pi K_i R \left( \left.\frac{\partial u}{\partial r}\right|_R - \frac{u}{R} \right) . \tag{3.9}$$

Therefore, the maximum time duration of the freezing stage $t_{mf}$, can be obtained by solving the following equation:

$$4\pi R^2 \delta R \rho_i (1 - I) L_f(0^{o}C) = \int_0^{t_{mf}} \left[ Q_V(u(R,t)) + 4\pi K_i R \left( \left.\frac{\partial u}{\partial r}\right|_R - \frac{u(R,t)}{R} \right) \right] dt. \tag{3.10}$$

If we find that

$$t_{mf} < \tau \tag{3.11}$$

where $\tau$ is the time duration of one full accretion cycle as determined by equation (2.1), then

$$t_f = t_{mf} . \tag{3.12}$$

If, on the other hand, it happens that

$$t_{mf} \geq \tau , \tag{3.13}$$

then

$$t_f = \tau \tag{3.14}$$

In this last case the cooling phase does not take place. From (3.8) the final temperature profile is

$$u(r,t_f) = \frac{2}{R} \sum_{n=1}^{\infty} \sin(\frac{n\pi r}{R}) \exp\left[\frac{-kn^2\pi t_f}{R^2}\right] \int_0^R f(\rho) \sin(\frac{n\pi\rho}{R})\, d\rho. \tag{3.15}$$

The time duration of the second phase, the cooling phase is given by

$$t_c = \tau - t_f . \tag{3.16}$$

During the cooling phase, the surface boundary condition is the following: the heat transfered from the hailstone to the environment must be equal to the heat flowing through its surface. The initial temperature profile for this stage is the final temperature profile of the freezing stage and is given by equation (3.15). This second

IBVP can be written formally as follows:

$$\frac{\partial u}{\partial t} = k \frac{\partial^2 u}{\partial r^2} \qquad 0 \le r \le R \tag{3.4}$$

$$u(0,t) = 0 \tag{3.17}$$

$$- 4\pi K_i R^2 \left.\frac{\partial T}{\partial r}\right|_R = - 4\pi K_i R \left( \left.\frac{\partial u}{\partial r}\right|_R - u(R,t) \right) = Q_{CC} + Q_{ES} \tag{3.18}$$

$$u(r,0) = f(r) = u(r,t_f) \tag{3.19}$$

Because $Q_{ES}$ depends on the saturation vapor pressure over the hailstone surface, which has a non-linear dependence on the temperature (exponential in $T^{-1}$ according to the Clausius-Clapeyron equation), this second IBVP is not a standard problem with well-known solutions. However, Macklin and Payne (1967) did linearize the boundary condition (3.18) by setting

$$\left.\frac{\partial T}{\partial r}\right|_R = - h_S (T_S - T_a) , \tag{3.20}$$

where $T_S$ is the hailstone surface temperature and $T_a$ is the air temperature. The proportionality constant $h_S$ is calculated by evaluating $Q_{CC}$ and $Q_{ES}$ (they actually used slightly different but equivalent expressions) using the deposit equilibrium temperature $T_d$ as obtained by the steady-state models and by dividing by the difference between this temperature and $T_a$:

$$h_S = \frac{Q_{CC}(T_d) + Q_{ES}(T_d)}{4\pi K_i R^2 (T_d - T_a)} . \qquad (3.21)$$

With this approximation the solution for the temperature can be written as (Carslaw and Jaeger, 1959)

$$T(r,t) = T_a + \frac{2}{Rr} \sum_{n=1}^{\infty} e^{-k\alpha_n^2 t} \frac{R^2\alpha_n^2 + (Rh_S - 1)^2}{R^2\alpha_n^2 + Rh_S(Rh_S - 1)} \sin \alpha_n r$$

$$\times \int_0^R (u(\rho,t_f) - \rho T_a) \sin\alpha_n\rho \, d\rho , \qquad (3.22)$$

where the $\alpha_n$ are the n roots of

$$R\alpha \cot R\alpha + Rh_S - 1 = 0 . \qquad (3.23)$$

As mentioned earlier in the discussion of the Macklin and Payne model in Chapter 1, it is difficult to evaluate the error introduced by linearizing the boundary condition. Furthermore, it is not necessary to look at solutions (3.7) and (3.22) in great detail to see that these cannot be of much practical use. Notations like $\Sigma$ and $\int$ are quite elegant, but getting actual numerical evaluations may require several approximations or simplifications which would have to be repeated for every point in time and space. In this case it seems just as well to calculate approximate solutions directly from the differential equation (3.4) together with the suitable boundary conditions. This is the approach taken in the proposed new

model: the partial differential equation (3.4) is approximated by means of finite differences.

## 3.2 Finite Differences and Grid Mesh

The simplest finite-difference approximation of the partial differential equation is given by the explicit marching form

$$\frac{u(r,t+\Delta t) - u(r,t)}{\Delta t} = k \frac{u(r+\Delta r,t) - 2u(r,t) + u(r-\Delta r,t)}{\Delta r^2} . \quad (3.24)$$

Therefore, if the values of u at points r, r - $\Delta$r, r + $\Delta$r are known at time t, it is possible to calculate u(r,t + $\Delta$t).

In order to be able to use the finite difference equation (3.24), the domain of solution has to be covered by a grid of points separated by space intervals $\Delta$t. In the new model the "size" of the domain of solution is changing constantly from accretion to accretion. The radius of the spherical hailstone increases with time, and the time duration of one cycle $\tau$ might increase or decrease depending on the relative variations of the terminal velocity $v_t$, and the liquid water content $w_f$ (see equation 2.1). Using the conventional notation

$$u_m^n = u(m\Delta r, n\Delta t), \quad (3.25)$$

equation (3.24) can be rewritten as

$$u_m^{n+1} = \lambda(u_{m-1}^n + u_{m+1}^n) + (1 - 2\lambda)\, u_m^n , \quad (3.26)$$

where

$$\lambda = \frac{k\Delta t}{\Delta r^2} . \tag{3.27}$$

Fourier component analysis of equation (3.26) yields the following stability condition

$$\lambda \leq \frac{1}{2} . \tag{3.28}$$

So once the radial interval $\Delta r$ has been fixed, there are severe limitations on the time interval $\Delta t$.

In the new model it was decided to use a constant number of radial divisions, so that the radial interval $\Delta r$ would increase from accretion to accretion. Preliminary trials were done with the explicit scheme (3.26). However, it was found that the method was extremely inefficient. Even when the largest $\Delta r$ possible for acceptable accuracy was used, constraint (3.28) was allowing only very small $\Delta t$, resulting in a very large number of time steps for one accretion cycle. Furthermore, in the cold parts of the cloud, in the dry growth regime, $t_f$ is much smaller than $t_c$ with the result that only a few time steps were available for the integration of the freezing phase, compared with a few thousand for the cooling phase. This was judged unacceptable, since from the heat budget standpoint the freezing part of the accretion cycle is just as important as the cooling part, and similar accuracy is needed in both. To remedy this problem, it was decided to resort to a more efficient implicit method.

## 3.3 The Crank-Nicholson Method

Another approximation to the partial differential equation (3.4) is given by

$$\frac{u(r,t+\Delta t) - u(r,t)}{\Delta t}$$

$$= k \frac{[u(r+\Delta r,t+\Delta t) - 2u(r,t+\Delta t) + u(r-\Delta r,t+\Delta t)]}{\Delta r^2} \quad (3.29)$$

Here the approximation of the second derivative is expressed at time $t + \Delta t$. The Crank-Nicholson method consists in using a linear combination of equation (3.24) and (3.29) to obtain the following formula:

$$(1-\gamma)\, u_{m+1}^{n+1} - [2(1-\gamma)\lambda + 1]\, u_m^{n+1} + (1-\gamma)\, u_{m-1}^{n+1}$$

$$= -\gamma\lambda u_{m-1}^n - (1 - 2\lambda\gamma)\, u_m^n - \gamma\lambda u_{m+1}^n , \quad (3.30)$$

where $\gamma$ is the weighting factor, and

$$0 < \gamma < 1 . \quad (3.31)$$

When $\gamma = 0$ we recover the explicit formulation (3.26).

Upon writing equation (3.30) for all values of $m = 0,M$, we are led to a tridiagonal system of $M - 1$ equations in $M - 1$ unknowns. The reason why there are only $M - 1$ unknowns at time $n + 1$ is because $u_0^{n+1}$ and $u_M^{n+1}$ are prescribed by the boundary conditions. In matrix form, the system of equations can be written

$$\begin{bmatrix} \beta & \alpha & & & \\ \alpha & \beta & \alpha & & \\ & \alpha & \beta & \alpha & \\ & & \ddots & \ddots & \ddots \\ & & & \alpha & \beta \end{bmatrix} \begin{bmatrix} u_1^{n+1} \\ u_2^{n+1} \\ \vdots \\ u_{M-1}^{n+1} \end{bmatrix}$$

$$= \begin{bmatrix} -\gamma\lambda u_o^n - (1 - 2\gamma\lambda)u_1^n - \gamma\lambda u_2^n - \alpha u_o^{n+1} \\ -\gamma\lambda u_1^n - (1 - 2\gamma\lambda)u_2^n - \gamma\lambda u_3^n \\ \vdots \\ -\gamma\lambda u_{M-2}^n - (1 - 2\gamma\lambda)u_{M-1}^n - \gamma u_M^n - \alpha u_M^{n+1} \end{bmatrix} \tag{3.32}$$

where

$$\alpha = (1 - \gamma)\lambda, \tag{3.33}$$

$$\beta = -[1 + 2(1 - \gamma)\lambda] . \tag{3.34}$$

This tridiagonal system can be solved easily by using the Thomas algorithm. For simplicity let us denote the M - 1 terms on the R.H.S. of system (3.31) by $d_m$. Using the transformation

$$c_1^* = \frac{\alpha}{\beta} , \tag{3.35}$$

$$d_1^* = \frac{d_1}{\beta} , \tag{3.36}$$

$$c_m^* = \frac{\alpha}{\beta - \alpha c_{m-1}^*}, \qquad m = 2,\ldots M-1, \tag{3.37}$$

$$d_m^* = \frac{d_m - \alpha d_{m-1}^*}{\beta - \alpha c_{m-1}^*}, \qquad m = 2, M-1, \tag{3.38}$$

we obtain,

$$u_{M-1}^{n+1} = d_{M-1}^* \tag{3.39}$$

$$u_m^{n+1} = d_m^* - c_m^* u_{m+1}^{n+1}, \qquad m = M-2, 1. \tag{3.40}$$

This scheme is stable for all $\lambda$ (Forsythe and Wasow, 1960).

## 3.4 An Iterative Boundary Condition

During the cooling stage of the accretion cycle, the amount of heat transferred to the atmosphere must be equal to the amount of heat flowing through the hailstone surface. This is the external boundary condition of the second IBVP,

$$-4\pi K_i R \left( \left.\frac{\partial u}{\partial r}\right|_R - \frac{u(R,t)}{R} \right) = Q_{CC} + Q_{ES}. \tag{3.18}$$

Writing this in finite difference form,

$$\frac{1}{R}\left[ \frac{u_M^{n+1} - u_{M-1}^{n+1}}{\Delta r} - \frac{u_M^{n+1}}{R} \right] = \frac{-(Q_{CC} + Q_{ES})}{4\pi R^2 K_i} = -Q^*, \tag{3.41}$$

$$u_{M-1}^{n+1} = u_M^{n+1} (1 - \Delta r/R) + R\Delta r Q^* . \qquad (3.42)$$

From equation (2.9), $Q_{ES}$ is directly proportional to the saturation vapor pressure over the hailstone surface, which depends on the surface temperature in a highly non-linear fashion. Equation (3.42) cannot be solved analytically in terms of $u_{M-1}^{n+1}$ to permit the use of the Thomas algorithm. Instead, an iterative method has to be used. Furthermore, it was found that a second order approximation of the surface derivative $\frac{\partial u}{\partial r}\Big|_R$ gave better results; perhaps this is because the finite difference approximation of the heat equation itself is of second order in r. Hence, we write:

$$\frac{\partial u}{\partial r}\Big|_R = \frac{3u_M^{n+1} - 4u_{M-1}^{n+1} + u_{M-2}^{n+1}}{2\Delta r} + O(\Delta r^2) . \qquad (3.43)$$

Upon substitution of this second order formulation in equation (3.41), we get

$$\frac{3u_M^{n+1} - 4u_{M-1}^{n+1} + u_{M-2}^{n+1}}{2\Delta r} - \frac{u_M^{n+1}}{R} = - RQ^* . \qquad (3.44)$$

Using the Thomas algorithm to get $u_{M-2}$ and $u_{M-1}$, substituting in (3.44) and rearranging, we get

$$\left( \frac{(3 - 2\Delta r/R)}{4 + c^{*}_{M-2}} + \frac{\alpha}{\beta - \alpha c^{*}_{M-2}} \right) u_M^{n+1} + \left( \frac{2R\Delta r}{4 + c^{*}_{M-2}} \right) Q^{*}$$

$$+ \frac{d^{*}_{M-2}}{4 + c^{*}_{M-2}} - \frac{A - \alpha d^{*}_{M-2}}{\beta - \alpha c^{*}_{M-2}} = 0 . \qquad (3.45)$$

Here,

$$A = - \gamma\lambda u^{n}_{M-2} - (1 - 2\cdot\lambda\gamma) u^{n}_{M-1} - \gamma\lambda u^{n}_{M} . \qquad (3.46)$$

Since $Q^{*}$ is actually a function of $u_M^{n+1}$, equation (3.45) contains only one unknown $u_M^{n+1}$, and it can be solved iteratively. In the model this is done by the method of false position (Sokolnikoff and Redheffer, 1966). Denoting the L.H.S. of (3.45) by F(x), the root of

$$F(x) = 0 , \qquad (3.47)$$

would be the proper value for $u_M^{n+1}$. Since the upper limit for $u_M^{n+1}$ is 0 (corresponding to the maximum temperature allowed in the model, $0^{o}C$), it can easily be shown that the following recurrence formula

$$x_{n+1} = \frac{x_n F(0)}{F(x_n) - F(0)} \qquad (3.48)$$

will converge to the root of (3.47). As a first guess for $x_n$ the value corresponding to a surface temperature equal to the air temperature is used since this is the lowest possible value of the surface temperature.

## 3.5 Stability with Respect to Heat Transfer

The duration of the freezing phase is determined by the amount of latent heat available from the freezing of the deposit. The time necessary for complete freezing is found by solving equation (3.10),

$$4\pi R^2 \delta R \rho_i (1 - I) L_f (0^{\circ}C) = \int_0^{t_{mf}} Q_v (u(R,t) + 4\pi K_i R \left( \frac{\partial u}{\partial r}\Big|_R - \frac{u(r,t)}{R} \right) dt \ . \tag{3.10}$$

Since we are using finite-difference methods, the R.H.S. of equation (3.10) becomes a summation:

$$\sum_{n=1}^{N} \left[ Q_v (u_M^n) + 4\pi K_i R \left( \frac{u_M^n - u_{M-1}^n}{\Delta r} - \frac{u_M^n}{R} \right) \right] \Delta t \ . \tag{3.49}$$

(Note that here N is the number that will make (3.49) equal to the L.H.S. of (3.10).) Unfortunately expression (3.49) proved quite difficult to handle as it was found to be very sensitive to the magnitude of $\Delta r$ and $\Delta t$. This is most likely due to the behaviour of the surface temperature gradient at the beginning of the phase. Initially, the surface temperature is raised suddenly at $0^{\circ}C$; this leads to an extremely large surface temperature gradient which decreases very rapidly afterwards. If an average of the initial and final temperatures for one time-step is used in an effort to get a better approximation to the average gradient, the estimated freezing time ($N\Delta t$) changes unpredictably when $\Delta r$ and $\Delta t$ are made smaller independently. This is basically due to the fact that the gradient itself decreases

exponentially with time (it can be easily seen that differentiation of (3.7) with respect to r does not affect the time dependence); therefore a simple average of the initial and final gradients, if those were exactly known, would always give an overestimate of the average gradient. On the other hand, in this case, the first order finite difference approximation always underestimates the surface gradient: so depending on the relative magnitude of $\Delta r$ and $\Delta t$ the internal heat fluxes would be underestimated or overestimated. A similar situation occurs when only the initial temperature for one time step is used. If the final temperature alone is used, the internal heat fluxes are always underestimated; but in order to attain a sufficient accuracy, $\Delta r$ and $\Delta t$ have to be so small that the advantages of using the Crank-Nicholson method are lost. In the search for a better way to estimate the internal heat fluxes, it was noticed that the temperatures themselves did not seem to be significantly affected by changes in $\Delta t$ and $\Delta r$. It was therefore decided to calculate how much the total heat content of the hailstone changed from one time-step to another. That is, at each time step, the total heat content is calculated and compared to the initial heat content to see how much heat has been conducted inside. This technique works quite nicely and although it requires more computation at each time iteration, this is more than compensated for by the fewer iterations needed with the Crank-Nicholson scheme. The increased accuracy of this method might also be explained by the fact that the total heat content is essentially calculated by adding the temperature at all the grid points, and its relative error remains of the same magnitude as that of the temperatures, whereas the

relative error of the surface gradient, which is essentially a difference of the temperatures can become intolerably high. (Note that even if the gradients might be very large due to very small $\Delta r$, the difference between two adjoining temperatures can be quite small.)

In the solution of the second IBVP of the second phase, when the change of the total heat content of the hailstone was compared to the heat that should have been transferred to the environment according to the surface temperature calculated from the boundary condition (3.43), a similar discrepancy occurred. Independent changes of $\Delta r$ and $\Delta t$ resulted in surface heat transfers, as calculated from (2.8) and (2.9), that were sometimes smaller, and sometimes larger than the internal heat changes, again in a rather unpredictable manner. However this time there seemed to be no possibility of avoiding the use of the surface temperature gradient. Although this problem might look similar to the one encountered in the first IBVP, it is different in the sense that we are not trying to estimate heat transfers from surface gradients during the span of one time-step. The surface temperature is found by equating the heat flux due to the gradient of temperature at the surface, to the fluxes to the atmosphere due to the surface temperature, at one particular instant. Although there may be some error in the approximation of the surface temperature gradient, the main cause of this problem is likely due to the method used to integrate the heat diffusion equation itself.

Indeed, the basis of the Crank-Nicholson scheme is that the rate of change of the temperature at one point during the time interval $\Delta t$ is set equal to the average of the finite difference approximation

of the laplacian of the temperatures expressed at time t and at time t + $\Delta t$; this should give a better representation of the average rate of change of the temperature during the time interval $\Delta t$, than the simple explicit formulation (3.23). However, from the theoretical solutions (3.7) and (3.21), we see that the temperature has an exponential "decrease" with time. Therefore as the length of a time step increases, a correspondingly greater weight should be given to the laplacian expressed at time t + $\Delta t$, in order to have a more accurate representation of the average rate of change of the temperature during the interval $\Delta t$. The original Crank-Nicholson method gives equal weight to the two laplacians. In order to remedy this problem the weighting factor $\gamma$ was set equal to

$$\gamma = \frac{1}{2 + \lambda} , \qquad (3.50)$$

where $\lambda$ is given by equation (3.26). Therefore as $\Delta t$ increases, $\gamma$ decreases and the weight is shifted towards the laplacian at time t + $\Delta t$. When $\Delta t$ decreases, $\lambda$ becomes smaller, and $\gamma$ tends towards 1/2, that is, equal weight is given to both laplacians. This method totally eradicated the wild fluctuations between the surface heat transfers and the internal heat changes, although some consistent error persisted. This error could be reduced at will by reducing $\Delta r$ and/or $\Delta t$. Since no improvement was obtained by expressing the surface gradient by an approximation of higher order than second order, it was decided that the remaining errors were simply truncation errors of the finite-difference approximation. Maybe an improvement

could be attained by devising a more clever $\gamma$, or by simply going to a more accurate scheme for the integration of the heat diffusion equation. However the present method is judged accurate enough for our purposes. Furthermore, according to Forsythe and Wasow (1970, p. 124) this method is stable and convergent, no matter how $\Delta t$ and $\Delta r$ tend to zero, when the weight given to the laplacian at time $t + \Delta t$ is equal to or greater than 1/2. This was amply verified in the many trials done to find a suitable combination of the number of time and space divisions.

# CHAPTER 4

## A FEW PROGRAMMING CONSIDERATIONS

### 4.1 Brief Description of Program

As previously mentioned, the model investigates the growth of a spherical hailstone under constant cloud conditions. The program is divided into three parts. The main program calculates the terminal velocity and the time duration of one cycle according to formulas (2.1) and (2.3). It also performs various other tasks like the calculation of the resulting ice fraction, the re-initialization of the grid after one cycle and the output of results. The solution to the heat diffusion equation is handled by two subroutines, FREEZ and COOL, depending on whether the hailstone is in the freezing stage or the cooling stage of the cycle. The mathematical methods used in these routines have been described in the previous chapter. A copy of the program is provided in Appendix 2. Calculations for 40 accretion cycles required about ten seconds of computing time on the Amdahl 470 at the University of Alberta.

## 4.2 Re-initialization After One Cycle

In this model, the number of grid points along a radius remains constant from cycle to cycle, and since the radius is becoming larger, the distance between two grid points is also increasing. Therefore from one cycle to another, the grid points do not correspond exactly. At the beginning of a cycle, immediately after the accretion of a new layer, the temperature is not known on the expanded grid, and it must be interpolated from the final temperature profile of the previous accretion. Let $\varepsilon$ be the displacement of a new grid point m, from its position before the accretion; then the temperature at this point $'u_m$ can be approximated by:

$$'u_m = u_m + \frac{(u_{m+1} - u_{m-1})}{2\Delta r} \varepsilon , \qquad (4.1)$$

where $u_m$ is the temperature at point M in the previous grid, and $\Delta r$ is the previous grid length. The displacement $\varepsilon$ is given by:

$$\varepsilon = \frac{m\delta R}{M} , \qquad (4.2)$$

where M is the total number of divisions, m the grid point number, and $\delta R$ the thickness of the accreted layer. At the surface point the temperature is set to $0^{\circ}C$, according to the model assumptions.

Some difficulties may arise however when the deposit thickness $\delta R$ is of the same order of magnitude as one space interval $\Delta r$. Figure 4.1 illustrates schematically what can happen when $\delta R$ is slightly greater than $\Delta r$. In this figure we see that the value at grid point

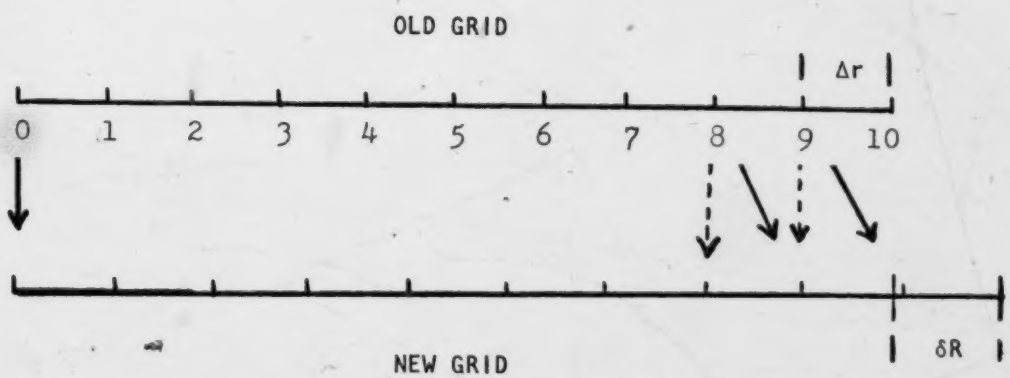


Figure 4.1 Problem of grid re-initialization when δR the deposit thickness is larger than Δr the grid point spacing.

7 (or 8) in the new grid would be better approximated by using estimates of the slope at grid points 8 (or 9) in the old grid, instead of at points 7 (or 8) as per equation (4.1). Nevertheless when the situation arose, total heat contents before and after the re-initialization were found to be within less than .05 percent of each other, indicating that procedure (4.1) was accurate enough for our purposes.

On the other hand, grid point 9 is now inside the accreted layer. In the model, if this situation were to occur, this grid point would also be initialized to $0^{o}C$ (indeed it was decided that whenever a grid point would be within .2 $\Delta r$ from the edge of the accreted layer, in the new grid, this grid point would also be initialized to $0^{o}C$); however during the integration of the heat diffusion equation for the freezing stage only the end point would be kept at $0^{o}C$ as a boundary condition.

## 4.3 Ice Fraction

When a hailstone enters the wet growth regime, the surface deposit freezes incompletely, because the surface heat fluxes are insufficient to get rid of all of the latent heat. This results in a new ice fraction I' which is calculated in the following manner:

$$I' = I + (1 - I)\, H_{TOT}/H_{max} , \qquad (4.3)$$

where I is the initial ice fraction of the deposit as given by (2.6), $H_{TOT}$ is the total heat that has been conducted inside the hailstone

and transferred to the environment, and $H_{max}$ is the maximum heat which could be available if the deposit were to freeze entirely.

In this regime, the surface temperature remains at $0^{o}C$, and the hailstone interior gradually warms up towards the melting point. After a certain time the internal temperature becomes uniform enough that it is meaningless to solve the heat diffusion equation. At this point the internal temperature gradients are so weak that the amount of heat conducted inside the hailstone becomes negligibly small compared to the other heat fluxes. The ice fraction is then basically determined by the external heat transfers alone and the model becomes essentially similar to the continuous models discussed in Chapter 1. It was decided (more or less arbitrarily) that this point is reached when the hailstone average temperature is equal to or greater than $-.001^{o}C$. Since the hailstone cannot become warmer than $0^{o}C$ this would correspond to a very weak gradient indeed.

## 4.4 Heat Content

As was discussed in Chapter 3, the easiest way to calculate how much heat has been conducted inside the hailstone is to evaluate the change in its total heat content. In our case the total quantity of heat $H_i$ contained in the stone is given by

$$H_i = \int_0^R c_i \, T(r) \, 4\pi r^2 \rho_i dr \qquad (4.4)$$

if we express $T(r)$ in degrees Celsius and make use of the function $u = rT$, we can define

$$H_i = 4\pi\rho_i c_i \int_0^R ru(r)dr \, . \qquad (4.5)$$

Therefore the heat content of a hailstone at $0^oC$ is zero, and it is negative for lower temperatures. In view of the initial assumptions, $\rho_i$ and $c_i$ are constant throughout the hailstone. The temperature is known at every grid point and integral (4.5) can be accurately approximated by the trapezoidal rule

$$\int_0^R u(r)rdr \simeq (\Delta r)^2 \sum_{m=1}^{M-1} mu_m^n + \frac{M}{2} u_M^n \qquad (4.6)$$

An interesting paradox arises in the calculation of the initial heat content, at the beginning of the freezing phase. Since in fact, the model accretes a deposit which is already at $0^oC$ (the heat of fusion released by the initial freezing having been used to warm the deposit), the total heat content of the hailstone is not changed, according to (4.5). However since the total mass of the hailstone has increased, the mean temperature has also increased and the hailstone is in fact warmer by the amount of heat that has been released during the initial freezing. Nevertheless this effect will have to be taken into consideration in the calculation of heat budgets.

## 4.5 Saturation Vapor Pressure

In order to calculate the heat transfers due to sublimation or evaporation of some of the deposit, it is necessary to calculate the vapor pressure at the hailstone surface and in the environment.

The model assumes that in the cloud the air is saturated with respect to a plane water surface at the environment temperature. This vapor pressure is calculated by Richard's method as formulated by Wigley (1974). The vapor pressure at the hailstone surface is assumed to be the saturation vapor pressure over a plane ice surface at the surface temperature, which is calculated by Lowe's polynomial approximation (1977).

## 4.6 Thermodynamic Constants

The value of the thermal diffusivity $k_i$ used in the integration of the heat diffusion equation is $1.09 \times 10^{-2}$ cm $^{o}C^{-1}$ $s^{-1}$ (since the program uses c.g.s. units) as proposed by Picca (1964); in SI units this is $1.09 \times 10^{-4}$ m $^{o}C^{-1}$ $s^{-1}$. The value of the thermal conductivity $K_i$ selected for the hailstone is $2.09 \times 10^{-4}$ W $m^{-1}$ $^{o}C^{-1}$ (.00500 c.g.s.) also as given by Picca. Measurements (Hobbs, 1974) indicate that it could vary between $2.5 \times 10^{-4}$ W $m^{-1}$ $^{o}C^{-1}$ and $2.0 \times 10^{-4}$ W $m^{-1}$ $^{o}C^{-1}$ over the temperature range $-30^{o}C$ to $0^{o}C$. A value of $1.46 \times 10^{-4}$ W $m^{-1}$ $^{o}C^{-1}$ (.0035 c.g.s.) was used by Goyer et al. (1969); however they claim that variations "over the physically reasonable range showed that the results were quite insensitive to this parameter".

Even though the heat capacity of ice can vary as much as 17 percent over the range of 0 - $-50^{o}C$, we are constrained by the assumptions of the model to keep it as a constant. In order to be consistent with equation (3.3) and the values selected above, the heat capacity of our theoretical hailstone was set at 2.09 J $kg^{-1}$

(.500 cal $g^{-1}$); .503 cal $g^{-1}$ is the specific heat capacity for ice at $0^{o}C$ given by the Smithsonian Meteorological Tables (List, 1958).

# CHAPTER 5

# RESULTS AND DISCUSSION

## 5.1 General Description

In this chapter, the model is used to investigate the growth of a hailstone in constant cloud conditions. Forty layers of 25 μm each are added to a spherical hailstone of radius 4.5 mm, resulting in a sphere of radius 5.5 mm. The details of these growth segments are calculated for six different sets of cloud conditions: for the first five sets, the stone is in the dry growth regime, and for the last one it enters the wet growth regime. These conditions are summarized in Table 5.1.

$T_i$, the initial constant temperature of the hailstone, was selected to correspond approximately to the equilibrium temperature $T_e$ as obtained from the continuous models for a hailstone of 5.0 mm radius. It can be seen from Figure 5.1 that the hailstone exhibits a fairly similar behaviour in all of the first five sets of cloud conditions. The final surface temperature for each cycle drops sharply after the first few accretions, then rises gently afterwards. Around accretion number 15, the hailstone seems to have reached some

Table 5.1

Environmental conditions for the investigated growth segments. P is the air pressure, $T_a$ the air temperature and $w_f$ the liquid water content. These conditions are consistent with the cloud model used by List et al. (1965). $T_i$ is the initial constant temperature of the hailstone and $T_e$ is the equilibrium temperature as obtained from List et al. (1965, 1967) model for a hailstone of 5.0 mm radius. The number in parenthesis is the ice fraction.

| Set | P(kPa) | $T_a$(°C) | $w_f$($10^{-3}$ kg $m^{-3}$) | $T_i$(°C) | $T_e$(°C) |
|---|---|---|---|---|---|
| a | 34.5 | -30 | 3.5 | -11.0 | -11.0 |
| b | 38.0 | -25 | 3.5 | -8.0 | -8.0 |
| c | 42.0 | -20 | 3.5 | -6.0 | -4.0 |
| d | 46.0 | -15 | 3.0 | -2.5 | -2.0 |
| e | 51.3 | -9 | 2.0 | -1.5 | -1.5 |
| f | 55.5 | -5 | 2.0 | -1.0 | 0.0(.75) |

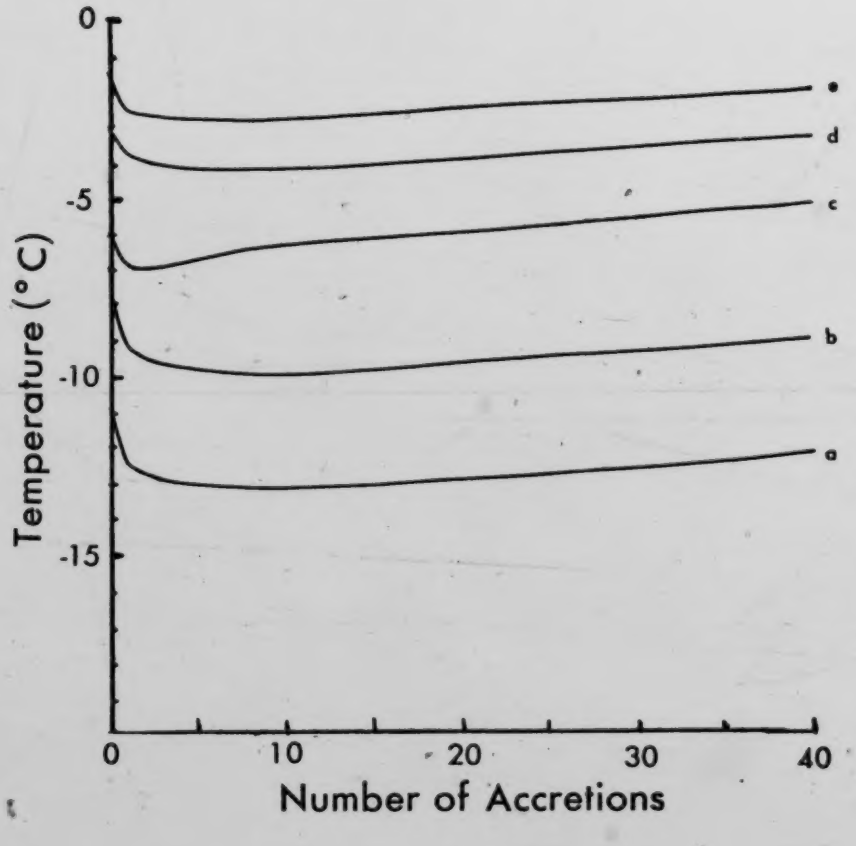


Figure 5.1 Final surface temperature of the hailstone after N accretions for different cloud conditions: a, b, c, d, e, (see Table 5.1). Note that continuous lines were drawn for ease of representation; each curve is obtained by joining a set of discrete points.

kind of equilibrium with the environment, and the slow rise of the final surface temperature can be attributed to the slowly increasing radius.

The slightly different aspect of curve c can be explained by the fact that the initial temperature $T_i$ is $2^{o}C$ cooler than the equilibrium temperature. For this reason the temperature starts to rise "sooner" than in the other cases, and ends up higher than the initial value after the full 40 accretions, also in contrast to the other cases.

For condition f, the hailstone enters the wet growth regime after the first accretion (Figure 5.2). The ice fraction drops sharply for a few accretions, again some sort of equilibrium after accretion number 10. Here also we did not select the equilibrium temperature as the initial condition in order to see how the equilibrium would be achieved, if this were the case.

At this point it should be made clear that the time scale for the realization of all the curves in Figure 5.1 and Figure 5.2 is different for each case. Because the hailstone is in different environmental conditions, its fall speed and its accretion rate are different. Table 5.2 gives a comparison of the elapsed time after the accretion of an equal number of layers for each case investigated.

Note that the time interval for the accretion of one layer decreases as the number increases; this is because a large hailstone has a faster rate of accretion than a smaller one, under the same environmental conditions. In Table 5.3, the final surface temperature for the twentieth accretion cycle is compared to the equilibrium

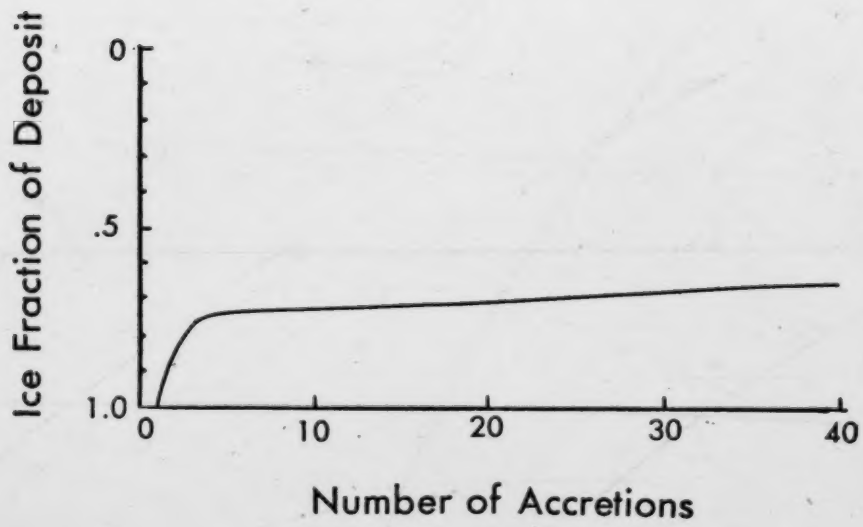


Figure 5.2 Ice fraction of surface deposit after N accretions of 25 μm layers, for cloud conditions f.

Table 5.2

Time necessary to accrete n layers of 25 μm for cloud conditions a, b, c, d, e and f.

| Number of Layers | Elapsed Time (s) | | | | | |
|---|---|---|---|---|---|---|
| | a | b | c | d | e | f |
| 1 | 1.25 | 1.30 | 1.35 | 1.64 | 2.56 | 2.65 |
| 2 | 2.50 | 2.60 | 2.71 | 3.27 | 5.12 | 5.29 |
| 3 | 3.75 | 3.89 | 4.05 | 4.90 | 7.67 | 7.92 |
| 4 | 4.99 | 5.18 | 5.40 | 6.52 | 10.22 | 10.55 |
| 5 | 6.23 | 6.47 | 6.74 | 8.14 | 12.75 | 13.16 |
| 10 | 12.37 | 12.86 | 13.38 | 16.18 | 25.33 | 26.15 |
| 20 | 24.23 | 25.38 | 26.41 | 31.94 | 50.01 | 51.63 |
| 30 | 36.18 | 37.59 | 39.13 | 47.31 | 74.08 | 76.48 |
| 40 | 47.66 | 49.52 | 51.74 | 62.32 | 97.58 | 100.74 |

Table 5.3

Comparison of the final surface temperature $T_{sf}$ after the 20th accretion cycle with the equilibrium temperature $T_e$ for a 5.0 mm hailstone under different cloud conditions. The number in parenthesis is the ice fraction.

| Cloud Conditions | a | b | c | d | e | f |
|---|---|---|---|---|---|---|
| $T_{sf}$ | -12.81 | -9.62 | -5.85 | -3.97 | -2.54 | 0(.70) |
| $T_e$ | -11.0 | -8.0 | -4.0 | -3.0 | -2.0 | 0(.75) |

temperature as obtained from the Listogram (Appendix 1) for each set of environmental conditions.

It is easily seen that for most cases $T_{sf}$ is significantly lower than the equilibrium temperature. The difference however decreases at higher temperatures. For conditions f both models result in the wet growth regime, and the ice fractions obtained are in reasonable agreement, considering the accuracy with which it can be read from the Listogram (Appendix 1).

## 5.2 A More Representative Temperature

The behaviour of the final surface temperature for each cycle does not permit one to draw any conclusions about the processes simulated by the model since this temperature is not representative of the hailstone during one accretion cycle. According to Figure 5.3 and Figure 5.4, there is quite a bit of variation near the surface, especially for cold conditions.

Figure 5.3 indicates that after the freezing phase, heat has penetrated further towards the center of the hailstone in warm conditions than in cold conditions. This is because it takes longer for the deposit to freeze in warm conditions. Since the surface is maintained at $0^{o}C$ for a longer period, there is more time for heat to diffuse inside. After the cooling phase, at the end of the accretion cycle, the temperature near the hailstone center is slightly warmer than at the beginning by typically a few tenths of a degree. However the surface temperature is significantly lower, as was

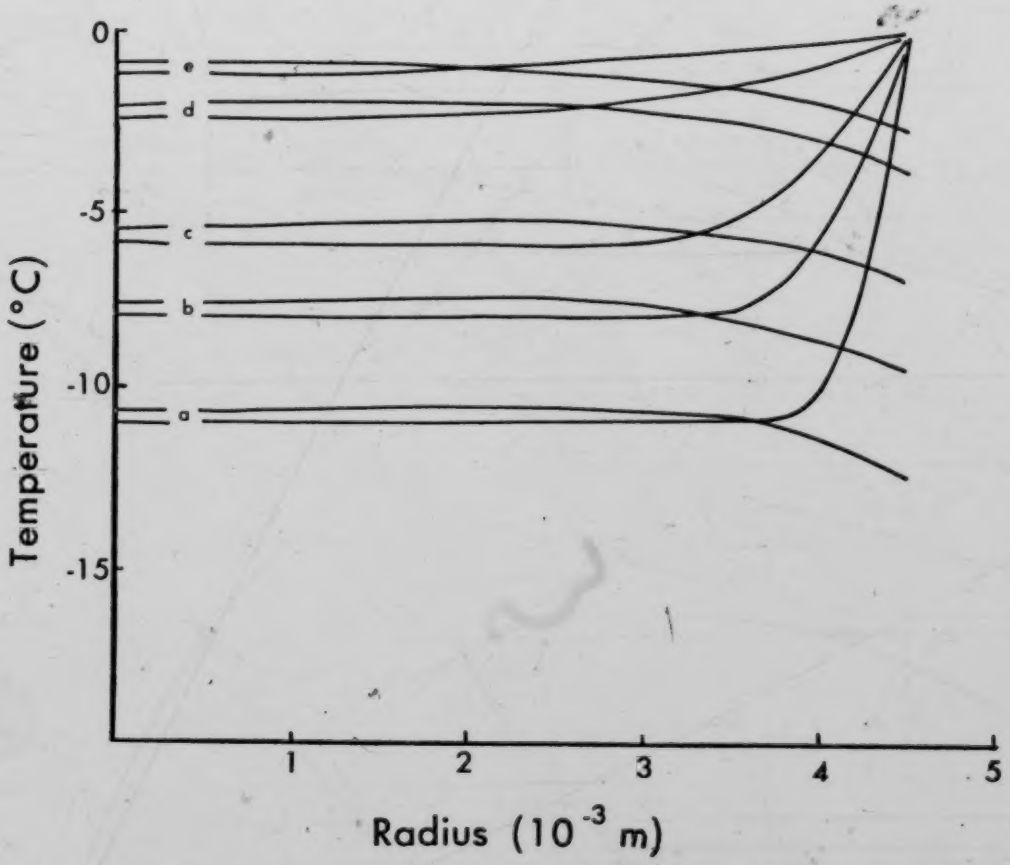


Figure 5.3 Internal temperature profiles for the first accretion cycle, after the freezing phase (those converging to $0^{o}C$) and after the cooling phase for cloud conditions a, b, c, d, e.

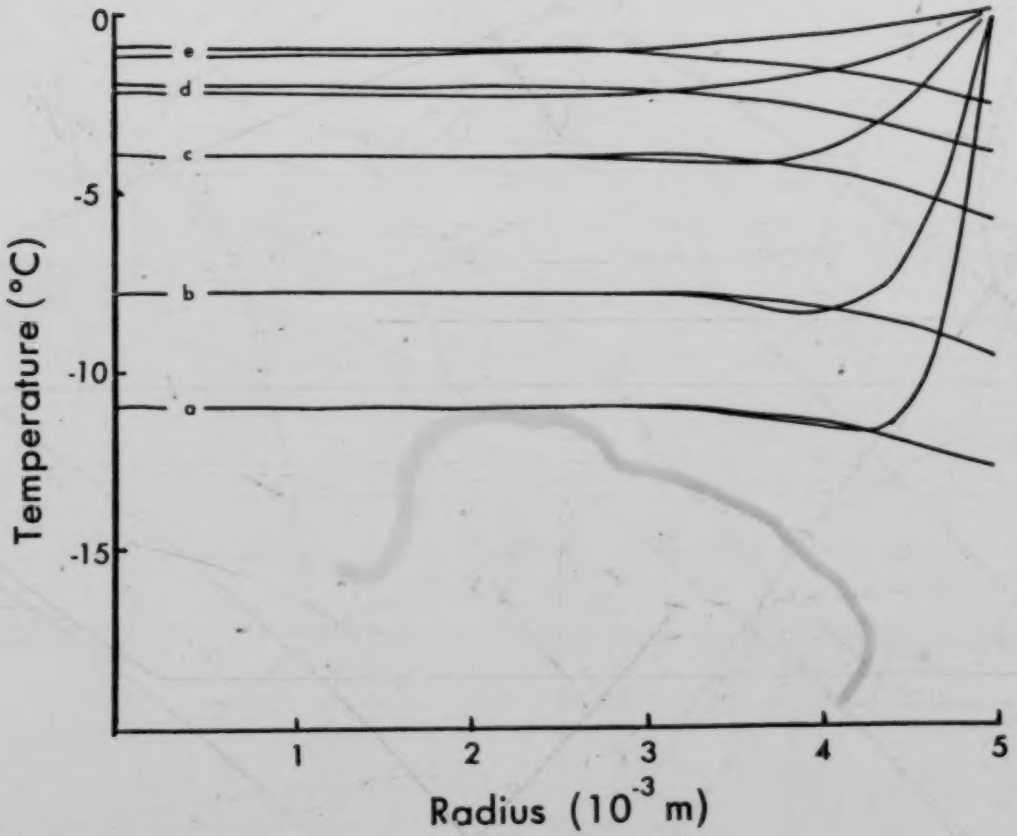


Figure 5.4 Internal temperature profiles for the twentieth accretion cycle, after the freezing phase and after the cooling phase.

observed in the previous section. It is interesting to note how similar in shape are each of the final temperature curves.

Figure 5.4 shows the same temperature profiles for the twentieth cycle. Here the temperature near the center remains virtually unchanged. Furthermore the depth of penetration (that is, the distance from the surface after which there is no significant temperature change) decreases for colder conditions. However it is still large enough to necessitate the consideration of spherical effects in the integration of the heat diffusion equation, which effects were neglected by Macklin and Payne (1967). Again the final temperature profiles are very similar in shape.

Figure 5.5 confirms our previous findings about large temperature fluctuations near the hailstone surface. We see that for conditions a, the hailstone spends about 65 percent of the time at a temperature lower than the equilibrium temperature $T_e$ obtained by the continuous models. As the cloud conditions become warmer, the hailstone spends a larger proportion of its time at a temperature above the corresponding $T_e$.

At this stage the need for a temperature that is more representative of what happens during one cycle is quite evident. For this purpose it was decided to calculate a time average of the temperature at each grid point for the duration of a cycle. Figure 5.6 gives the profiles of such average temperatures for the first accretion. It is quite noticeable that all the curves are fairly uniform, although exhibiting generally a slight fall towards the center of the hailstone. Also all curves with the exception of

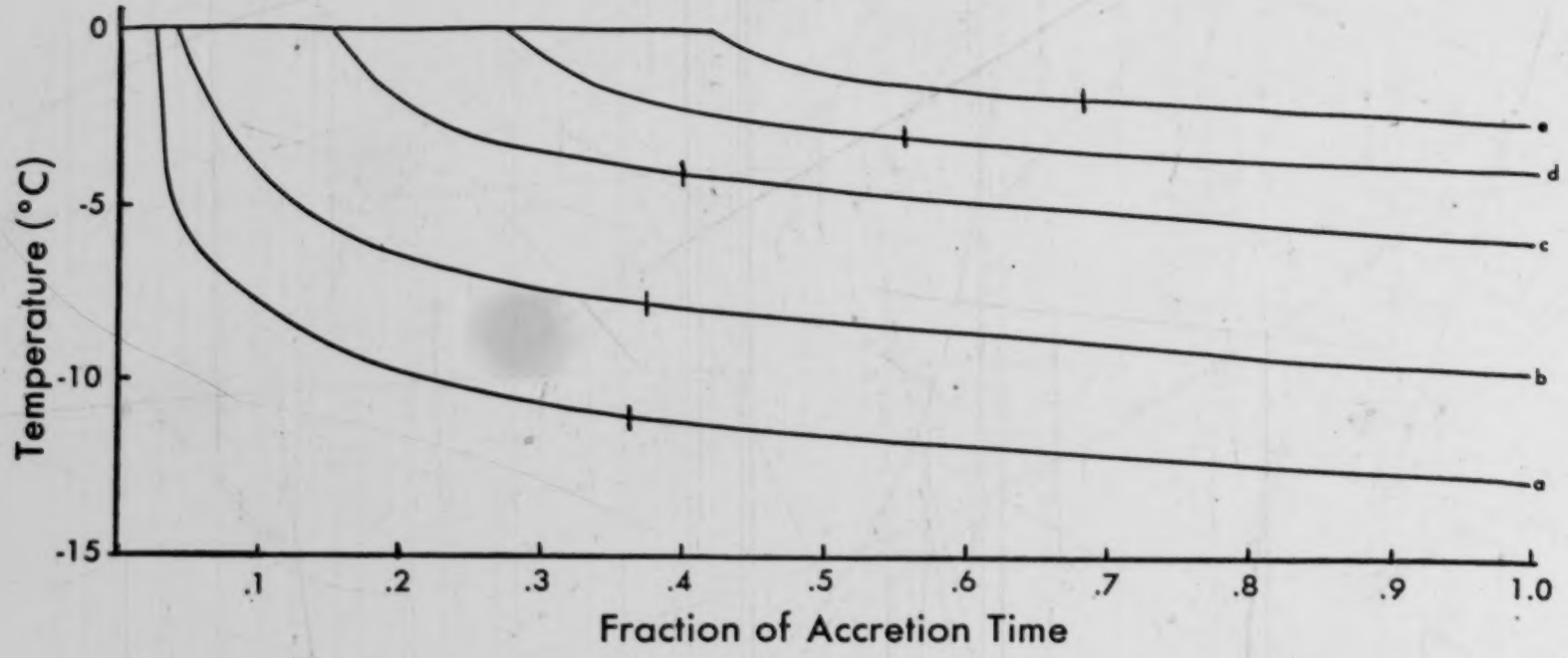


Figure 5.5 Surface temperature as a function of time, during accretion number 20 for cloud conditions a, b, c, d, e.

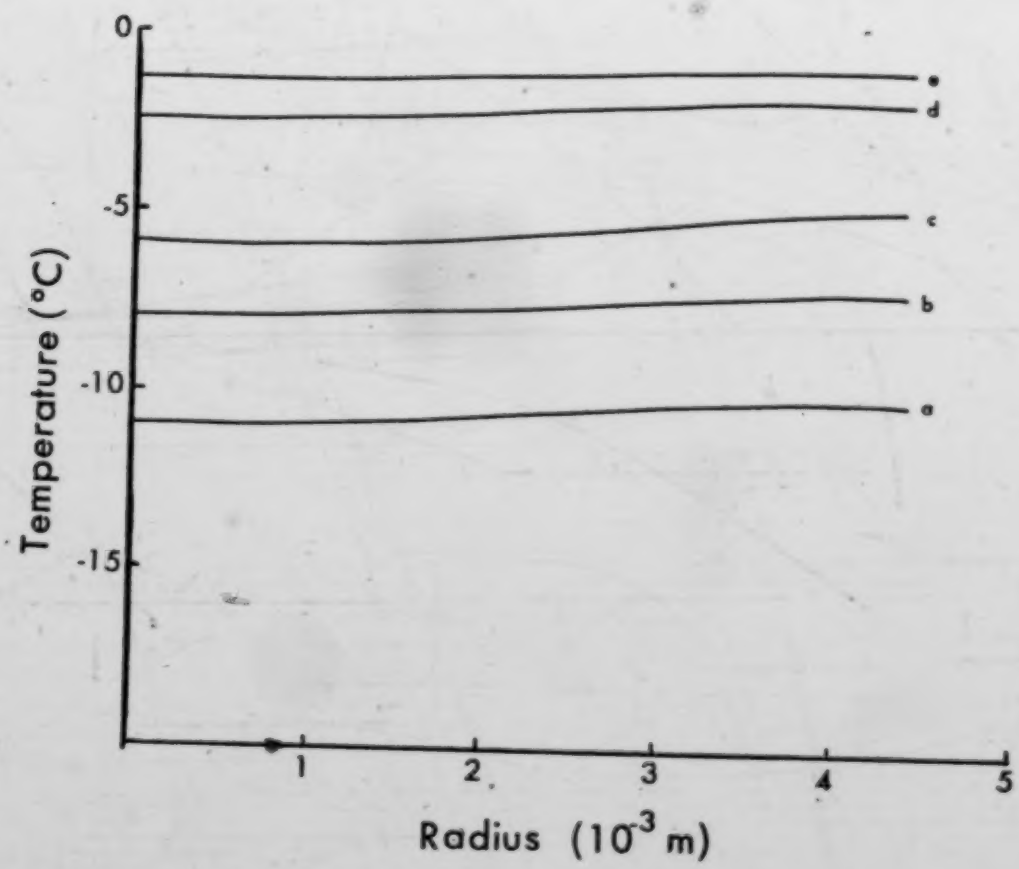


Figure 5.6 Time averaged temperature profiles during the first accretion, for all of the dry growth conditions.

curve c (because of the lower initial conditions) have a slight maximum which is close to the surface, but away from it, indicating that the surface heat flux was on the average out of the hailstone.

By the time the hailstone reaches the twentieth accretion cycle, its average internal temperature is very uniform. From Table 5.4 we see that in all cases there is a slight temperature drop from the surface to the center, about one-tenth of a degree, indicating that the hailstone is warming slowly on the average because of its increasing radius. However, essentially, the hailstone has a constant average temperature which is indistinguishable from the equilibrium temperature obtained by the continuous model. Therefore it seems as if the hailstone adjusts itself to a new thermodynamic equilibrium in such a manner that its average temperature is the same as the temperature predicted by the continuous models.

## 5.3 The Mechanism of Equilibrium

It was mentioned in section 5.1 that after the first accretion, the final surface temperature is significantly lower than the initial temperature; also this effect is more pronounced for colder conditions (see Figure 5.1). Similar results were obtained by Macklin and Payne (1967), although they seemed somewhat surprised by these findings. They thought that the cooling phase would terminate when the surface temperature returned to the initial temperature, and that this would happen when all the heat conducted internally during the freezing phase had been transferred back to the environment. But this is impossible and the reason is very simple indeed. Since

Table 5.4

Average temperature ($^{o}$C) at different points along the hailstone radius, for the twentieth accretion cycle, under different cloud conditions. $T_e$ is the corresponding equilibrium temperature from List et al. (1965) model.

| Distance from Center (cm) | Cloud Conditions | | | | |
|---|---|---|---|---|---|
| | a | b | c | d | e |
| .05 | -10.91 | -7.67 | -3.94 | -2.17 | -1.08 |
| .10 | -10.91 | -7.67 | -3.94 | -2.16 | -1.08 |
| .15 | -10.90 | -7.67 | -3.93 | -2.16 | -1.07 |
| .20 | -10.90 | -7.66 | -3.93 | -2.16 | -1.07 |
| .25 | -10.89 | -7.65 | -3.92 | -2.15 | -1.07 |
| .30 | -10.88 | -7.64 | -3.90 | -2.15 | -1.06 |
| .35 | -10.86 | -7.63 | -3.89 | -2.14 | -1.06 |
| .40 | -10.85 | -7.61 | -3.87 | -2.12 | -1.05 |
| .45 | -10.83 | -7.59 | -3.84 | -2.10 | -1.04 |
| .50 | -10.82 | -7.57 | -3.81 | -2.08 | -1.03 |
| $T_e$ | -11.0 | -8.0 | -4.0 | -2.0 | -1.5 |

by hypothesis, the surface temperature is raised to 0°C during the freezing phase, this means that part of the hailstone interior will warm up and the internal temperature will rise (see Figure 5.3). When the hailstone enters the cooling phase, its surface temperature falls faster and becomes lower than the temperature at some point inside (otherwise there would be no heat flow out of the hailstone). As a result, when the hailstone surface returns to the initial temperature, at some point inside, the temperature has to be warmer than the initial value. It is therefore physically impossible for all the heat that has been injected into the hailstone during the freezing phase to have been transferred back to the environment at that point.

We find that the surface returns to the initial temperature fairly early during the cycle (Figure 5.5 is a good indicator although not exactly representative of the first cycle) and that the hailstone ends up colder than initially after the cycle is fully completed. This is because the amount of heat conducted into the hailstone during the freezing phase is significantly lower than the amount of heat transferred back to the environment during the cooling phase. Intuitively, however, we know that if the external conditions are kept constant, the hailstone cannot keep cooling forever, accretion after accretion. There must come a stage where the heat transfers will adjust themselves to try to balance on the whole.

In Table 5.5 we see how this process takes place. During the first few accretions there is a net cooling of the hailstone which causes a lower final surface temperature; this in turn causes sharper internal gradients at the beginning of the next accretion resulting in

Table 5.5

Energy budgets of each accretion cycle for cloud condition a. $H_i$ is the heat conducted to the hailstone during the freezing stage; $H_o$ is the heat transferred to the environment during the cooling stage; $H_d$ is heat released by the cooling of the deposit (see text); W is the net warming of the hailstone.

| m | $H_i$(J) | $H_o$(J) | $H_d$(J) | W(J) |
|---|---|---|---|---|
| 1 | 1.09 | 1.40 | .15 | -.16 |
| 2 | 1.13 | 1.37 | .15 | -.09 |
| 3 | 1.14 | 1.36 | .16 | -.06 |
| 4 | 1.15 | 1.36 | .16 | -.05 |
| 5 | 1.16 | 1.37 | .16 | -.05 |
| 6 | 1.17 | 1.37 | .17 | -.03 |
| 7 | 1.19 | 1.39 | .17 | -.03 |
| 8 | 1.21 | 1.40 | .17 | -.02 |
| 9 | 1.22 | 1.40 | .17 | -.01 |
| 10 | 1.23 | 1.41 | .18 | .00 |
| 11 | 1.25 | 1.41 | .18 | .02 |
| 12 | 1.26 | 1.42 | .18 | .02 |
| 13 | 1.27 | 1.43 | .18 | .02 |
| 14 | 1.29 | 1.44 | .18 | .03 |
| 15 | 1.30 | 1.45 | .18 | .03 |
| 16 | 1.31 | 1.46 | .19 | .04 |
| 17 | 1.33 | 1.47 | .19 | .05 |
| 18 | 1.34 | 1.48 | .19 | .05 |
| 19 | 1.36 | 1.50 | .19 | .05 |
| 20 | 1.37 | 1.51 | .19 | .05 |

a stronger internal heat flow. Therefore it becomes apparent that the hailstone attempts to adjust its temperature cycle in order to reach a final temperature profile such that the heat which flows inside during the next freezing phase will be balanced by the heat that flows out during the subsequent cooling phase. Unfortunately the process of achieving equilibrium is further complicated by the fact that the hailstone is growing and that the accretion rate (and therefore the rate of heat release), increases with the hailstone radius faster than the cooling rate (see Chapter 2). This is why there is a point of turnaround near accretion number 20 and why the hailstone warms up slowly thereafter.

We will now explain in greater detail how the budgets of Table 5.5 were calculated. $H_i$ is the amount of heat that was conducted into the hailstone during the freezing phase; it is equal to the latent heat released by the freezing of the remaining water in the deposit after the initial freezing, and is given by equation (2.7). $H_o$ is the amount of heat that has been transferred from the hailstone to the environment. This can be calculated by using equations (2.19) and (2.20) in conjunction with the surface temperature at every timestep, or by evaluating the difference in the hailstone heat content at the beginning and at the end of the cooling phase. Both methods were used and it was found that values obtained with the first method were consistently higher than the values obtained by the second method by a little less than 2 percent. However, as mentioned in the discussion of section 3.5, this was judged to be an acceptable error.

A slight difficulty arises because of the procedure used to

calculate the hailstone heat content. The total heat content of the hailstone remains unchanged when the deposit is instantaneously accreted on it, although the hailstone is in fact warmer (because of a higher average temperature as discussed in section 4.4). Since the deposit is maintained at $0^{o}C$ throughout the freezing phase, none of its heat could diffuse into the stone interior, and only the latent heat released has affected the total heat content. However, during the cooling phase heat is removed from the deposit also, and this is debited against the total heat content of the hailstone. Therefore in order to obtain the net warming, the heat released by the cooling of the deposit, $H_d$ in Table 5.5, must either be added to the heat conducted to the hailstone ($H_i$), or subtracted from $H_o$.

Table 5.6 gives the net hailstone warming for one cycle at a selected number of accretions for all other dry growth conditions. Clearly the hailstone exhibits a similar behaviour in each case (with the exception of case c) and by the twentieth accretion an equilibrium is attained.

## 5.4 An Hypothesis

Let us return to Figure 5.5 and examine one curve in particular, say curve b. This curve registers the surface temperature of the hailstone for the twentieth accretion cycle. However, instead of assuming that the deposit has been accreted all at once, let us consider that it is being formed of individual cloud droplets arriving on the surface at short regular time intervals. A droplet that had just arrived on the surface would have just entered the freezing phase and

Table 5.6

Net hailstone warming in Joules, for one accretion after a selected number of accretions. These are for cloud conditions b, c, d, and e (see Table 5.1).

| n | b | c | d | e |
|---|---|---|---|---|
| 1 | -.13 | +.03 | -.13 | -.13 |
| 5 | -.03 | +.07 | .00 | -.01 |
| 10 | +.02 | +.07 | +.03 | +.03 |
| 15 | +.04 | +.06 | +.04 | +.03 |
| 20 | +.05 | +.06 | +.05 | +.04 |

would have a temperature of 0°C; but a droplet that had arrived one full period $\tau$ earlier would presumably be at the end of the cooling phase and would have reached the final temperature. Similarly a droplet accreted half a period ago would have cooled to a temperature of about -8.5°C. Since on the average, droplets should cover the entire hailstone surface within one period $\tau$, one could make the hypothesis that curve b represents the areal distribution of temperature for a hailstone of 5 mm radius, at equilibrium, growing in environmental conditions b (see Table 5.1). Of course such reasoning could also be applied to curves a, c, d, and e.

Unfortunately, there are several objections against this hypothesis. The first one, and undoubtedly the most important, is that our calculations assume radial heat transfers. If droplets are to be considered individually, lateral heat transfers would have to be taken into account: so one cannot just simply assume that individual droplets would have a temperature cycle identical to that of a uniform deposit. A second objection lies with the statistical nature of the accretion process. It is very unlikely that the hailstone will be covered uniformly by the droplets; more likely droplets will overlap in some portions of the surface while they will be late in covering some other regions. (And we won't even think about possible splashing or bouncing of the droplets!)

It would be very difficult to assess quantitatively the total effect of these processes. Considering the freezing phase, for example, it would appear that the lateral heat transfers might shorten the freezing time. On the other hand, the presence of several droplets

at different temperatures over the hailstone should have a tendency to smooth out the internal temperature gradients; this could have the opposite effect of reducing the freezing rate. Alternatively, during the cooling phase, a droplet could be affected differently depending on whether it happens to be in an area where the majority of the droplets are at a colder or warmer stage of their cycle.

Keeping those objections in mind, let us nevertheless go ahead with the hypothesis that Figure 5.5 gives the areal temperature distribution of a growing hailstone in equilibrium at different cloud conditions. Several interesting characteristics of the hailstone thermodynamic state can be estimated from this hypothetical temperature distribution. The most obvious is of course the mean surface temperature; this in fact corresponds to the time average of the surface temperature already discussed in section 5.2 and found to be essentially equal (within a few tenths of a degree) to the equilibrium temperature obtained by the continuous models.

A second important parameter of the temperature distribution is the standard deviation. It gives a better idea of the spread of the surface temperatures about the mean, which is not quite obvious just by looking at Figure 5.5. Such standard deviations were calculated for the five cloud conditions leading to dry growth for a 5 mm hailstone and are plotted in Figure 5.7. When the hailstone reaches the wet growth regime, the model yields a uniform temperature of $0^{o}C$, with a zero standard deviation. This is why the curve goes through the origin. An interesting feature of this graph is the weak dependence of the standard deviation on the mean surface tempera-

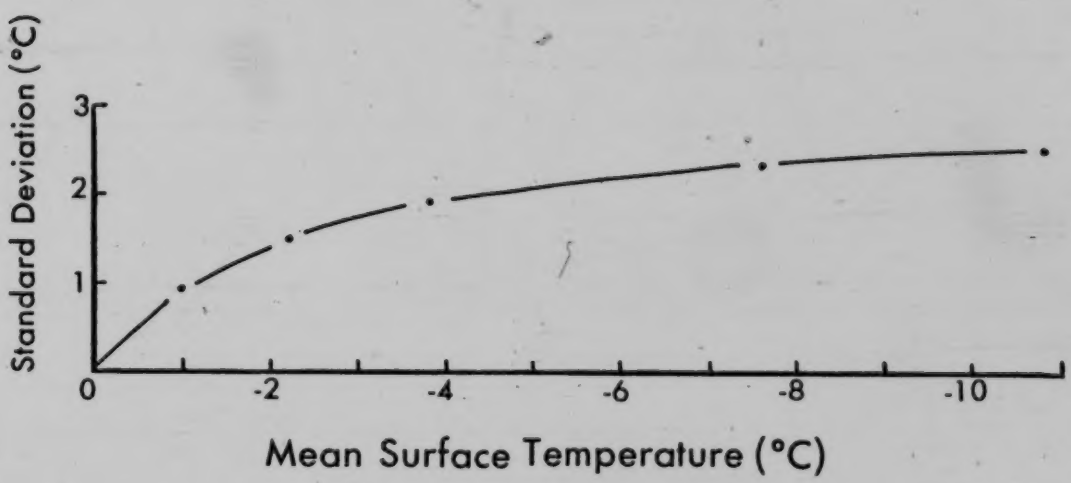


Figure 5.7 Standard deviation of the surface temperature distribution as a function of the mean temperature of the hailstone surface for a 5 mm radius hailstone.

ture. For temperatures colder than $-2^{o}C$, the standard deviation is $2^{o}C \pm .5^{o}C$.

By calculating the ratio of the freezing time to the total duration of one cycle, an estimate of the proportion of the surface which is in the wet growth regime can be obtained. This has been plotted in Figure 5.8. It can be easily seen that the "fractional wet growth area" has a very strong dependence on the surface temperature. These results would also support the suggestion that the transition from the dry to wet growth regimes is not discontinuous as implied by the continuous models, but occurs relatively smoothly as the mean surface temperature rises towards the melting point.

## 5.5 Effect of Deposit Thickness

In order to investigate possible effects of the thickness of the accreted deposit, the calculations were done again using deposits of thickness 5, 10 and 50 μm for cloud conditions a and d. It was found that in each case the hailstone undergoes a temperature cycle fairly similar to the one described in the previous sections. Furthermore, according to Table 5.7, the hailstone soon reaches a state of equilibrium in which the average temperature rises gradually due to its slowly increasing radius. Also, at equilibrium, the average temperature is essentially equal for all layers, the maximum difference being less than $1^{o}C$ from the largest to the smallest layer under condition a. However, according to Table 5.8 there is a significant dependence of the final surface temperature after one accretion cycle upon the deposit thickness.

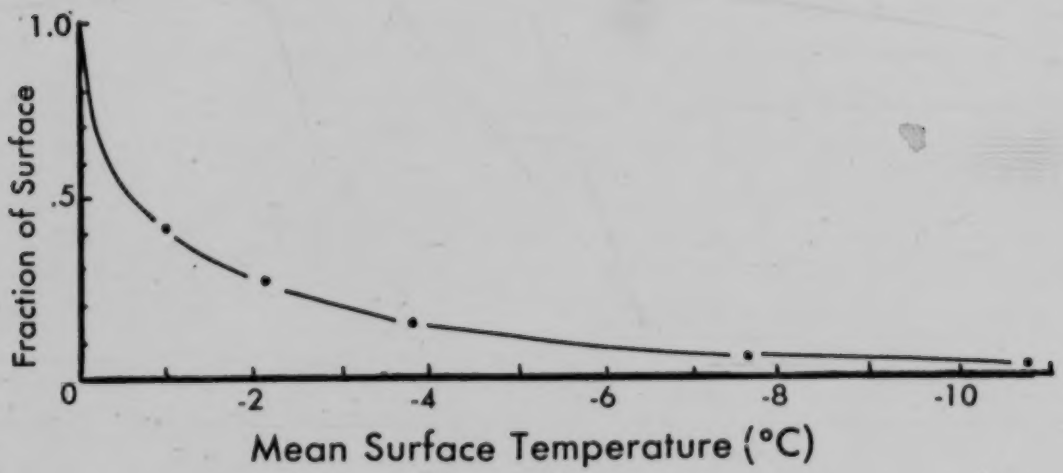


Figure 5.8 Fraction of the surface in the wet growth regime as a function of the mean surface temperature. This is obtained by calculating the ratio of the freezing time to the total time of one accretion cycle for a hailstone of 5 mm radius.

Table 5.7

Time averaged surface temperature over one accretion cycle, at selected hailstone sizes, for different deposit thicknesses, under cloud conditions a and b. The starting radius is 4.5 mm for the 25 and 50 μm layers and 4.8 mm for the 5 and 10 μm layers.

| δR | 5 μm | 10 μm | 25 μm | 50 μm |
|---|---|---|---|---|
| R(mm) | | (a) | | |
| 4.55 | - | - | -10.93 | -9.87 |
| 4.80 | -10.63 | -10.40 | -11.01 | -10.96 |
| 4.90 | -10.34 | -10.61 | -10.94 | -10.96 |
| 5.00 | -10.08 | -10.47 | -10.82 | -10.90 |
| 5.10 | -9.89 | -10.32 | -10.70 | -10.80 |
| 5.20 | -9.73 | -10.19 | -10.55 | -10.68 |
| | | (b) | | |
| 4.55 | - | - | -2.07 | -1.64 |
| 4.80 | -2.21 | -1.94 | -2.28 | -2.21 |
| 4.90 | -2.19 | -2.14 | -2.21 | -2.20 |
| 5.00 | -2.06 | -2.04 | -2.08 | -2.08 |
| 5.10 | -1.93 | -1.93 | -1.97 | -1.98 |
| 5.20 | -1.80 | -1.80 | -1.85 | -1.87 |

Table 5.8

Final surface temperatures after one accretion cycle at selected hailstone sizes, for different deposit thicknesses δR, under cloud conditions a and b. The starting radius is 4.5 mm for the 25 and 50 μm layers, and 4.80 mm for the 5 and 10 μm layers.

| δR | 5 μm | 10 μm | 25 μm | 50 μm |
|---|---|---|---|---|
| R (mm) | | | | |
| | | (a) | | |
| 4.55 | - | - | -12.99 | -13.06 |
| 4.80 | -11.56 | -11.82 | -13.00 | -13.82 |
| 4.90 | -11.25 | -11.88 | -12.93 | -13.80 |
| 5.00 | -10.99 | -11.74 | -12.81 | -13.73 |
| 5.10 | -10.79 | -11.57 | -12.67 | -13.63 |
| 5.20 | -10.63 | -11.45 | -12.55 | -13.48 |
| | | (b) | | |
| 4.50 | - | - | -4.01 | -4.33 |
| 4.80 | -3.13 | -3.20 | -4.18 | -4.82 |
| 4.90 | -3.09 | -3.38 | -4.09 | -4.77 |
| 5.00 | -2.95 | -3.28 | -3.97 | -4.64 |
| 5.10 | -2.82 | -3.16 | -3.83 | -4.52 |
| 5.20 | -2.67 | -3.04 | -3.70 | -4.39 |

Table 5.9 compares the accretion of deposits of different thicknesses for an equivalent radial increment, starting with the same initial conditions. When the hailstone reaches 4.60 mm, just about the same amount of heat has been conducted to the interior, regardless of whether the accretion consists of two 50 μm layers or four 25 μm layers. However, in the first case, a little less than twice as much time is spent in the freezing phase. Because of this the hailstone spends more time at 0°C and the total amount of heat transferred to the environment is somewhat larger when only two 50 μm layers are accreted. This explains the slightly lower final hailstone average temperature.

However the main reason for the difference in the final surface temperature revealed in Table 5.8 can best be explained by considering Figure 5.9. When the first 50 μm layer is accreted about 2.4 J are conducted inside the hailstone in about .15 s. When the first 25 μm layer is accreted about half of that amount of heat, roughly 1.3 J, is conducted inside during about one-quarter of the time (see Table 5.9). This means that, proportionately, the heat given to the hailstone in the last case is much closer to the surface, readily available to be transferred back to the atmosphere during the cooling phase (upper diagrams of Figure 5.9). When the 50 μm layer is about halfway through the cooling phase, the surface is again raised to 0°C in the other case, by the addition of another 25 μm layer (middle diagrams). Consequently there is more heat close to the surface, available for the next cooling period, and the surface temperature does not lower as much as for the 50 μm layer (lower diagrams). In other words, the difference in final surface temperature

Table 5.9

Comparison of accretion cycles for cloud condition a, starting with a 4.5 mm radius hailstone at -11°C, adding (i) two 50 μm layers; (ii) four 25 μm layers. $t_f$ is the freezing time, $\tau$ the accretion time. $H_f$ heat conducted inside during $t_f$, $H_o^{-1}$ heat transferred to the environment during $t_f$, $H_o^2$ heat transferred to the environment during the cooling phase, $\theta$ the mass average of the hailstone final temperature after one cycle.

| R | $t_f$(s) | r(s) | $H_1$(J) | $H_o^1$(J) | $H_o^2$(J) | $\theta$(°C) |
|---|---|---|---|---|---|---|
| | | | (i) | | | |
| 4.55 | .1544 | 2.50 | 2.42 | .370 | 2.80 | -11.57 |
| 4.60 | .1236 | 2.48 | 2.47 | .314 | 2.76 | -11.91 |
| TOTALS | .2780 | 4.98 | 4.89 | .684 | 5.56 | |
| | | | | 6.24 | | |
| | | | (ii) | | | |
| 4.525 | .0419 | 1.25 | 1.20 | .119 | 1.42 | -11.22 |
| 4.55 | .0353 | 1.25 | 1.21 | .0848 | 1.40 | -11.35 |
| 4.575 | .0342 | 1.25 | 1.22 | .0829 | 1.40 | -11.46 |
| 4.60 | .0336 | 1.24 | 1.24 | .0822 | 1.40 | -11.55 |
| TOTALS | .145 | 4.99 | 4.87 | .369 | 5.62 | |
| | | | | 5.99 | | |

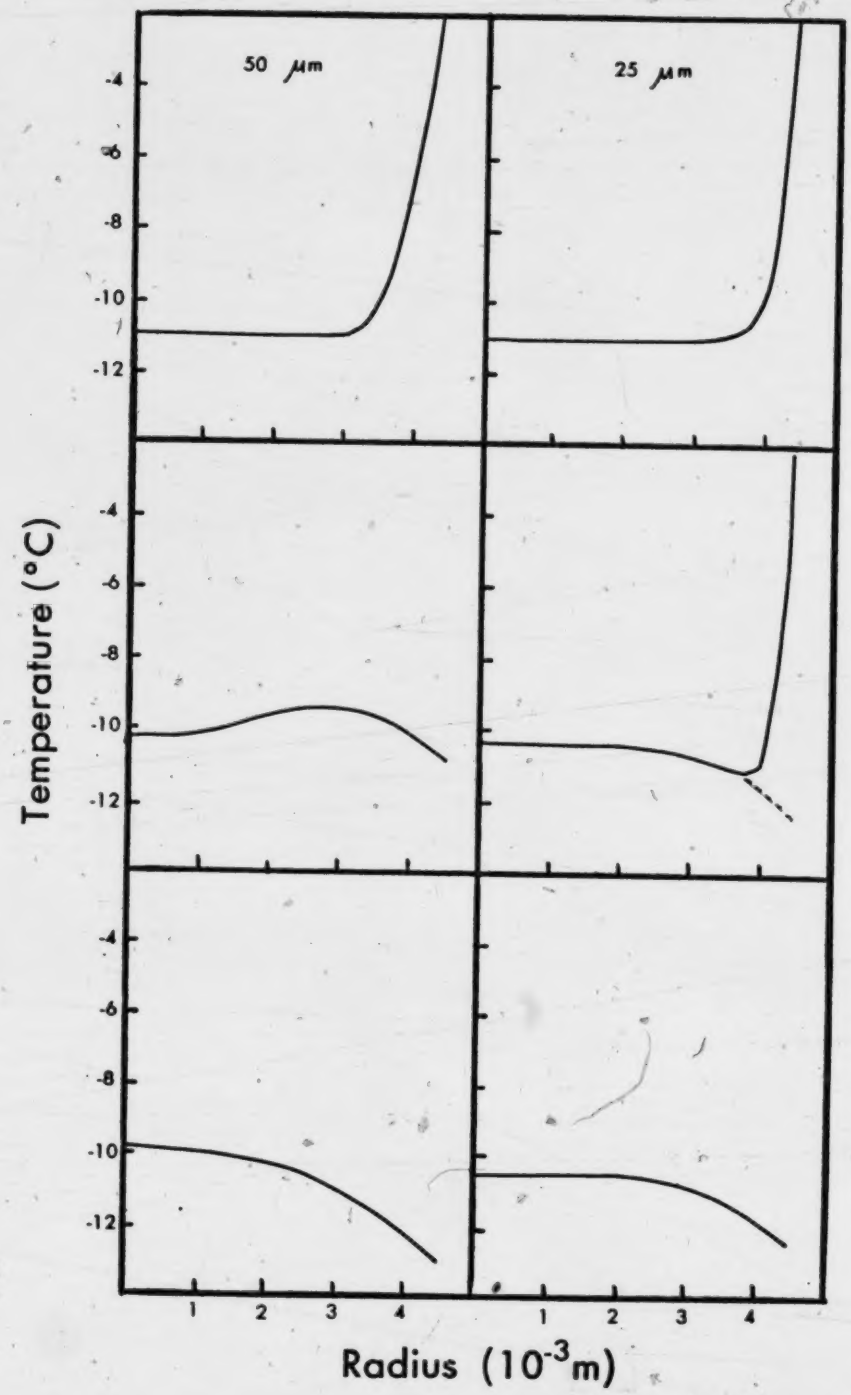


Figure 5.9 Hailstone temperature profiles during a 50 μm growth. The left diagrams are for the accretion of one 50 μm layer; the right diagrams two 25 μm deposits. In both cases the initial conditions are a hailstone of 4.5 mm radius at -11°C in cloud condition a.

is due to the combined effects of raising the surface temperature to $0^{o}C$ more frequently with a larger number of small layers, and to the time lag required for the heat to diffuse back and forth inside the hailstone.

The net effect of reducing (increasing) the thickness of the accreted deposit is to reduce (increase) the range of the surface temperature variations. Therefore returning to the hypothesis that the time cycle of the surface temperature can be viewed as the areal distribution of temperature over the hailstone, the effect should be reflected in the calculated standard deviation. In terms of such an interpretation the thickness of the deposit should correspond to the thickness of the droplets after their accretion (droplets do spread upon accretion; Macklin and Payne, 1967) on the hailstone. Figure 5.10 gives a plot of the standard deviation as a function of the thickness. As was shown in Figure 5.7, the standard deviations are slightly less under condition d, compared to condition a, indicating a weak dependence on the hailstone mean surface temperature. The two curves also indicate that the dependence on the accreted deposit thickness (or the size of the accreted droplets) is not very strong either, with a tendency to become even weaker for larger thicknesses. This is easily understood since the surface temperature cannot become lower than the air temperature nor higher than $0^{o}C$, which puts a limit to the range of the temperature cycle. The reason for having the standard deviation go to zero is to indicate how this discrete model and the continuous model could merge together, in the limit of an infinitesimal deposit. The limiting process could be visualized in the following

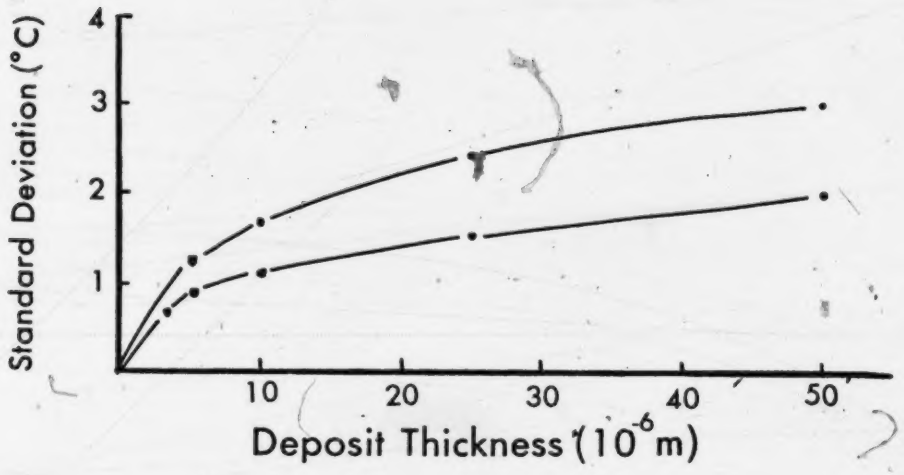


Figure 5.10 Standard deviation of the surface temperature distribution as a function of deposit thickness (or droplet thickness after accretion) for cloud conditions a (upper curve) and b (lower curve).

manner. The infinitely small deposit (or accreted droplet) is warmed up to 0°C instantaneously, and cools back to the mean temperature in an infinitesimally short time. An additional calculation with a deposit thickness of 2.5 μm for condition d (plotted in Figure 2.10) seems to support this idea.

Unfortunately, there is no simple way in which the above results can be related to the size of the cloud droplets before accretion. Macklin measured experimentally the spreading of supercooled droplets freezing on an ice surface and found a very strong dependence on the temperature of the accreting surface (see Macklin and Payne, 1967), with the larger spreadings occurring at warmer temperatures. Other factors found to be of lesser importance were the speed of impaction, and the initial temperature of the droplets.

Table 5.10 gives the droplet radius required to form a deposit of 25 μm in thickness for a given mean surface temperature, as calculated by Macklin's method (Macklin and Payne, 1967). As can be seen droplets about three times larger are needed when the surface is about -1°C, compared to -11°C. For the same mean temperature, when the other factors affecting droplet spreading are neglected, there is a linear relationship between the deposit thickness and the droplet radius before accretion. Therefore the conclusion to be tentatively drawn from Table 5.11 would be that a hailstone growing in conditions of large cloud droplets would have a "broader" surface temperature distribution than the same hailstone growing in a region where cloud droplets are smaller, other things being equal.

Table 5.10

Droplet radius required to form a 25 μm surface deposit, for different mean surface temperatures. Calculations were done using Macklin's method (Macklin and Payne, 1967).

| $T_M$(°C) | -1.03 | -2.08 | -3.81 | -7.57 | -10.82 |
|---|---|---|---|---|---|
| r(μm) | 170 | 150 | 120 | 75 | 60 |

Table 5.11

Standard deviation σ of the surface temperature distribution for different cloud droplets radii before accretion (calculated using Macklin's method). Calculations are for cloud conditions a and d.

| Cloud condition a | | | | |
|---|---|---|---|---|
| σ(°C) | 1.22 | 1.68 | 246 | 3.20 |
| r(μm) | 12 | 24 | 60 | 120 |

| Cloud condition d | | | | | |
|---|---|---|---|---|---|
| σ(°C) | .69 | .89 | 1.11 | 1.47 | 1.78 |
| r(μm) | 15 | 30 | 60 | 75 | 300 |

The effect of thickness was also investigated for the wet growth regime. No detectable influences appeared in the results as the calculated ice fractions were identical to the ones plotted in Figure 5.2, regardless of whether the deposit thickness was 5, 10, or 50 μm. This confirms the conclusion reached earlier in section 4.3 that this discrete model becomes essentially similar to the continuous models when internal conduction becomes negligible.

## 5.6 Freezing Times

One of the fundamental assumptions of our model (after Macklin and Payne, 1967) is that the time of initial freezing is so short that it is negligible compared to the time of subsequent freezing, and that no heat is exchanged outside the deposit during this first phase. As discussed in Chapter 1, the velocities for ice growth in freezing supercooled cloud droplets are not available; in order to obtain estimates of these velocities we use the linear crystalization velocities as a function of supercooling of Figure 1.1. Ratios of the estimated initial freezing time to the subsequent freezing time are given in Table 5.12. According to these values the initial assumption seems well justified.

It might be more difficult to try to estimate the possible heat exchanges from the droplet during this phase. If we assume that the heat transfers due to forced ventilation calculated at $0^{o}C$ would constitute an upper limit (the droplet should have an average temperature lower than $0^{o}C$ during this phase), then the ratio of the heat transfers during the two phases would be less than the ratios of the

Table 5.12

Ratio of the estimated initial freezing time $t_i$ to the subsequent freezing time $t_f$ for different cloud conditions and mean surface equilibrium temperatures $T_e$. While this ratio is estimated to be an upper limit for the ratio of heat transferred to the environment, the square root of the ratio is estimated to be an upper limit for the heat conducted to the hailstone in both phases.

| Cloud Conditions | $T_e$ | $t_i/t_f$ | $\sqrt{t_i/t_f}$ |
|---|---|---|---|
| a | -10.82 | .0040 | .062 |
| b | -7.57 | .0025 | .050 |
| c | -3.81 | .0013 | .036 |
| d | -2.08 | .0010 | .031 |
| e | -1.03 | .0012 | .035 |

times. From Table 5.9 we find that the amount of heat conducted to the hailstone during the freezing phase is roughly proportional to the square root of the time for which the surface is maintained at 0°C. Again it seems realistic that the extrapolation of this relationship to the initial freezing would yield an upper limit to the amount of heat conducted from the droplet to the underlying surface. Therefore the ratio of the heat conducted in both phases would be proportional to the square root of the time ratio, which is also given in Table 5.12. Values are typically about 5 percent. It might be argued that this is not exactly negligible, thereby weakening the validity of our assumption. On the other hand, heat transfers outside the deposit are not simply disregarded. What our assumption does is to delay their realization till the subsequent freezing and assume that they occur at 0°C. But the effect of the delay is immaterial since the initial freezing time is neglected. Actually, what could happen, is that some of the heat would be conducted into the hailstone before the deposit reaches 0°C, thereby reducing the internal gradients and, perhaps, reducing the total amount of heat conducted into the hailstone. But certainly this effect would be much less than what is indicated in Table 5.12.

# CHAPTER 6

## SUMMARY AND CONCLUSIONS

Results show that even with the temperature cycle imposed by the model, the hailstone soon reaches a state of equilibrium in which the time average temperature is essentially equal to the equilibrium temperature as calculated by the continuous models. It is also found that the net effect of allowing internal conduction is negligible, yielding only a very slight average temperature gradient due to the slow rise of the surface average temperature of the growing hailstone. However, within one accretion cycle there exists large heat fluxes of the same magnitude, but opposite in direction which have a determinating influence on the duration of the freezing phase and the overall time dependence of the surface temperature. Indeed, the surface temperature cycle adjusts in such a way as to try to balance the heat conducted to the hailstone during the freezing phase, with the heat transferred to the environment during the cooling phase.

Under the hypothesis that individual droplets accreted by the hailstone would have a temperature cycle similar to the uniform deposit used in the model, an estimate of the temperature distribution over the hailstone surface can be obtained. From such a

distribution, the mean surface temperature, the standard deviation and the fractional area of wet growth can be calculated. While the mean temperature is essentially equal to the equilibrium temperature of the continuous models, the standard deviation shows a weak dependence on the mean surface temperature and on the thickness of the droplets after accretion. From the fractional area of wet growth we see that the transition from the dry to the wet growth regimes occur fairly smoothly when the mean surface temperature rises towards $0^{o}C$, and not in a discontinuous fashion, as implied by the continuous models.

Although it is very difficult to analyze quantitatively the validity of the above hypothesis, qualitatively it can be argued that the overall effects of lateral heat transfers and lateral temperature gradients would not change the freezing times or standard deviations to a very large extent. The stochastic nature of the accretion process has not been considered in this work. It is our feeling, however, that the possibility of overlapping and coalescence of accreted droplets over some area of the hailstone, combined with the fact that cloud droplets distribution is not monodisperse, would have a tendency to broaden the temperature distribution.

As a final conclusion, this model lends more support to the claim (Macklin and Payne, 1967; Pellet and Dennis, 1974) that the equilibrium temperature obtained from the continuous models is an adequate representation of the hailstone temperature. However this new model has the advantage of providing a simple estimate of the temperature distribution over the hailstone surface, which indicates that if the cloud droplets size distribution has little effect on the

mean surface temperature, it has some influence on the standard deviation.

## BIBLIOGRAPHY


American Institute of Physics Handbook, 1972, D.E. Gray Editor, McGraw-Hill.

Bilham, E.G. and E.F. Relf, 1937: The Dynamics of Large Hailstones. Quart. J. Roy. Meteor. Soc., Vol. 63, 149-162.

Browning, K.A. and F.H. Ludlam, 1962: Airflow in Convective Storms. Quart. J. Roy. Meteor. Soc., Vol. 88, 117-135.

Carslaw, H.S. and J.C. Jaeger, 1959: Conduction of Heat in Solids. Clarendon.

Changnon, S.A., 1971: Economic Losses from Hail in the United States. Preprints of the Seventh Conference on Severe Local Storms, Kansas City, Missouri.

Forsythe, G.E. and W. Wasow, 1960: Finite Differences Methods for Partial Differential Equations. Wiley.

Goyer, G.G., S.S. Lin, S.N. Gitlin and M.N. Plooster, 1969: On the Heat Transfers to Ice Spheres and the Freezing of Spongy Hail. J. Atmos. Sci., Vol. 26, 319-326.

Hitschfeld, W. and M. Stauder, 1967: The Temperature of Hailstones. J. Atmos. Sci., Vol. 24, 293-297.

Hobbs, P.V., 1974: Ice Physics. Clarendon.

Kuo-Nan Lion, 1976: On the Absorption, Reflection and Transmission of Solar Radiation in Cloudy Atmospheres. J. Atmos. Sci., Vol. 33, 798-805.

List, R., 1963: General Heat and Mass Exchange of Spherical Hailstones. J. Atmos. Sci., Vol. 20, 189-197.

_____, P.H. Schuepp and R.G.J. Methot, 1965: Heat Exchange Ratios of Hailstones in a Model Cloud and their Simulation in a Laboratory. J. Atmos. Sci., Vol. 22, 710-718.

_____ and J.G. Dussault, 1967: Quasi Steady State Icing and Melting Conditions and Heat and Mass Transfer of Spherical and Spheroidal Hailstones. J. Atmos. Sci., Vol. 25, 522-529.

List, R., P.I. Joe, P.R. Kry, M.R. deQuervain, P.Y.K. Lui, P.W. Stagg, J.D. McTaggart-Cowan, E.P. Lozowski, M.C. Steiner, J. Von Niederhausen, R.E. Stewart, E. Freire, G. Lewis, 1976: Loss of Accreted Water from Growing Hailstones. Preprints of the International Conference on Cloud Physics, Boulder, Colorado, 255-269.

List, R.J., 1958: Smithsonian Meteorological Tables. The Smithsonian Institute.

Lowe, P.R., 1977: An Approximating Polynomial for the Computation of Saturation Vapor Pressure. J. Appl. Meteor., Vol. 16, 100-103.

Ludlam, F.H., 1950: The Composition of Coagulation - Elements in Cumulonimbus. Quart. J. Roy. Meteor. Soc., Vol. 76, 52-58.

_____, 1951: The Heat Economy of a Rimed Cylinder. Quart. J. Roy. Meteor. Soc., Vol. 77, 663-666.

_____, 1958: The Hail Problem. Nubila, Vol. 1, 13-96.

Macklin, W.C., 1962: Density and Structure of Ice Formed by Accretion. Quart. J. Meteor. Soc., 30-56.

_____ and B.F. Ryan, 1965: The Structure of Ice Grown in Bulk Supercooled Water. J. Atmos. Sci., Vol. 22, 452-459.

_____ and G.S. Payne, 1967: A Theoretical Study of the Ice Accretion Process. Quart. J. Roy. Meteor. Soc., Vol. 93 195-213.

Pellet, J.L. and A.S. Dennis, 1974: Effects of Heat Storage in Hailstones. Preprints of the Conference in Cloud Physics, Tucson, Arizona, 63-66.

Picca, R., 1964: Conduction de la chaleur a l'interieur d'un grêlon sphérique. Journal de Recheches Atmosphériques, Vol. 1, 51-53.

Reif, F., 1965: Fundamentals of Statistical and Thermal Physics. McGraw-Hill.

Schumann, T.E.W., 1938: The Theory of Hailstone Formation. Quart. J. Roy. Meteor. Soc., Vol. 64, 3-21.

Sokolnikoff, I.S. and R.M. Redheffer, 1966: Mathematics of Physics and Modern Engineering. McGraw-Hill.

Strong, G.S., 1974: The Objective Measurement of Alberta Hailfall. M.Sc. Thesis, University of Alberta.

Wigley, T.M.L., 1974: Comments on "A simple but accurate formula for the saturation vapor pressure over liquid water". J. Appl. Meteor., Vol. 13, 608.

# APPENDIX 1

## LISTING OF PROGRAM

```
      COMMON/BLOCK1/U(101,6)/ITEMS/ETF,FFLUX,IR,IT,
     *R,TIM,ENMAX,TF,ENDIS(2) ,RINC
      REAL LWC
      DOUBLE PRECISION U
      READ(5,100)RINC,R,KMAX,IWRITE
      IR=100
      READ(5,200)TA,P,TO,LWC
      II=IR+1
      DR=(R+RINC)/IR
      DO 10 K=1,II
10    U(K,1)=TO*(K-1)*DR
20    U(1,2)=0.
      ELTIM=0.
      CWBAR=1.0035+.005*EXP(.693*(273-TA)/10.)
      IF(TA.LT.253.)C12=.235
      IF(TA.GT.273.)C12=.207
      IF(TA.GE.253..AND.TA.LE.273.)C12=.207+.0014*
     *(TA-253.)
      FLUX=(1.44E-03*((TA*P)**.25)*(273-TA)+28.03*
     *C12*((TA**(.1))/(P**.75)*(6.107-VAP(TA))))
      RLF=79.7-CWBAR*(273.-TA)
C
C
C     START ACCRETING CYCLE
C
      DO 1 K=1,KMAX
      DO 11 N=1,II
      U(N,5)=0.
11    U(N,6)=0.
      R=R+RINC
      DR=R/IR
      VT=3705.*SQRT(TA*R/P)
      TIM=3.668*RINC/(VT*LWC)
      ELTIM=ELTIM+TIM
      FICE=CWBAR*(273-TA)/79.7
      ENMAX=73.1*(1.-FICE)*RINC
      FFLUX=FLUX*.118/R**.25
      IF(IR.EQ.1)GOTO150
      IF(U(II,1).GE.-.1E-05)U(II,1)=-.1E-05
      ETF=RLF*RINC*R/U(II,1)
      ETF=343.*ETF*ETF
      IT=50
C
C
C    INITIATE FREEZING CYCLE
C
      CALL FREEZ (I1,I2,&150)
      IF(TF.GE.TIM)GOTO 59
```

```
C    INITIATE COOLING CYCLE
C
       TC=TIM-TF
       IC=TC/TIM*100
       IF(IC.GT.50)IC=50
       IF(IC.EQ.0)GOTO 59
       CALL COOL (IR,IC,TC,TIM,C12,TA,P,R,I1,I2)
C
C
C    CALCULATE RESULTING ICE FRACTION
C
       DFICE=1.
       GOTO 60
59     DFICE=FICE+(1.-FICE)*ENDIS(I2)/ENMAX
60     CONTINUE
       IF(MOD(K,IWRITE).GT.0)GOTO 7
C
C
C    OUTPUT OF RESULTS
C
       WRITE(6,300)TIM,ELTIM,DFICE,ETF
       RR=0.
       DO 8 N=3,II,2
       RR=(N-1)*DR
       TEMP=U(N,I2)/RR
       IF(IC.EQ.0)U(N,4)=0.
       TEMP1=U(N,4)/RR
       ATEMP=(U(N,5)*TF+U(N,6)*TC)/TIM/RR
       TEMPF=U(N,3)/RR
       WRITE(6,400)RR,TEMPF,TEMP1,TEMP,ATEMP
8      CONTINUE
       IF(K.NE.KMAX)WRITE(6,600)
7      CONTINUE
C
C
C    REINITIALIZATION OF THE GRID AFTER ACCRETION
C    OF ANOTHER LAYER
C
       DO 9 N=2,IR
9      U(N,I1)=(U(N+1,I2)-U(N-1,I2))*RINC*(N-1)/
      *(2.*IR*DR)+U(N,I2)
        U(II,I1)=U(II,I2)*(R+RINC)/R
       IF(I1.EQ.1)GOTO 1
       DO 12 N=1,II
12     U(N,1)=U(N,I1)
       GOTO 1
150    DFICE=FICE+(1.-FICE)*FFLUX*TIM/ENMAX
       WRITE(6,300)TIM,ELTIM,DFICE
1      CONTINUE
       STOP
```

```
100    FORMAT(2F10.8,4I5)
200    FORMAT(3F10.5,F10.9)
300    FORMAT(1H ,'FALL TIME',F7.2,5X,'ELAPSED TIME'
      *,F7.2,5X,'DEPOSIT ICE FRACTION',F5.2,E12.4)
400    FORMAT(1H ,1F10.5,4F11.3)
600    FORMAT(1H1)
       END
```

```
C   THIS FUNCTION CALCULATES THE SATURATION VAPOUR
C   PRESSURE WITH RESPECT TO WATER ACCORDING TO
C   WIGLEY'S METHOD JAM, 13, P. 608.
C
      FUNCTION VAP(T)
      TH=1.-373/T
      X1=TH
      X2=X1*TH
      X3=X2*TH
      A=13.3185*X1-1.976*X2-.6445*X3-.1299*X3*TH
      VAP=1013.25*EXP(A)
      RETURN
      END
```

```
C    THIS SUBROUTINE SOLVES THE HEAT EQUATION WITH
C    THE SURFACE TEMPERATURE MAINTAINED AT 0C UNTIL
C    THE SURFACE DEPOSIT IS ENTIRELY FROZEN.
C    THE CRANK-NICHOLSON METHOD IS USED.
C
C
      SUBROUTINE FREEZ (I1,I2,*)
      COMMON/BLOCK1/U(101,6)/ITEMS/ETF,FFLUX,IR,
     *IT,R,TIM,ENMAX,TF,ENDIS(2),RINC
      DIMENSION CSTAR(500),DSTAR(500)
      DOUBLE PRECISION U,CSTAR,DSTAR,ALM,GAM,DR2,
     *HCO,HCT
      DR=R/IR
      IH=.5*IT
       DT=ETF/IT
      IF(ETF.GE.TIM)DT=TIM/IT
      IF(ETF.GE.TIM/2.)IH=1
      ALM=.0109*DT/(DR*DR)
      BETA=ALM/(ALM+2.)
      ALM=ALM*(1.-1./(2.+ALM))
      ENDIS(1)=0.
      ENDIS(2)=0.
C
C
C   CALCULATE THE INITIAL HEAT CONTENT
C
C
      DR2=DR*DR
      HCO=0.
      DO 22 N=2,IR
22    HCO=HCO+(N-1)*U(N,1)
      HCO=(HCO+IR*U(IR+1,1)/2.)*DR2
      HCO=HCO-RINC*U(IR+1,1)*R
      IF(HCO/(4.189*R*R*R).GE.-.001)GOTO 150
      HCO=.45*HCO/(R*R)
       GAM=-ALM*2.-1.
      MLIM=2*IT
      CSTAR(1)=ALM/GAM
C
      U(IR+1,1)=0.
      FK=RINC/DR+.2
      IK=FK
       IF(IK.EQ.0)GOTO 45
      DO 44 J=1,IK
44    U(IR+1-J,1)=0.
45    CONTINUE
```

```
C    START TIME ITERATIONS
C
C
      DO1 M=1,MLIM
      TP=M*DT
      I2=MOD(M,2)+1
      I1=I2-1
      IF(I1.EQ.0)I1=2
C
C
C     CALCULATE THE TRANSFORMED COEFFICIENTS BY THE
C     THOMAS ALGORITHM
C
C
      DSTAR(1)=-(U(2,I1)*(1.-2.*BETA)+BETA*U(3,I1))
     */GAM
      II=IR-1
      DO 2 I=2,II
      CSTAR(I)=ALM/(GAM-ALM*CSTAR(I-1))
2     DSTAR(I)=(-(U(I+1,I1)*(1.-2.*BETA)
     *+BETA*(U(I,I1)+U(I+2,I1)))
     *-ALM*DSTAR(I-1))/(GAM-ALM*CSTAR(I-1))
C
C
C     CALCULATE VALUES AT GRID POINTS
C
C
      U(IR,I2)=DSTAR(II)
      U(IR+1,I2)=0.
      U(IR,5)=U(IR,I2)+U(IR,5)
      U(IR+1,5)=U(IR+1,I2)+U(IR+1,5)
      DO3 N=2,II
      U(IR+1-N,I2)=DSTAR(IR-N)-CSTAR(IR-N)*
     *U(IR+2-N,I2)
3     U(IR+1-N,5)=U(IR+1-N,5)+U(IR+1-N,I2)
      IF(M.LE.IH)GOTO 1
C
C
C     CALCULATE RESULTING HEAT CONTENT
C
C
      HCT=0.
      DO 33 N=2,IR
33    HCT=HCT+(N-1)*U(N,I2)
      HCT=(HCT+IR*U(IR+1,I2)/2.)*DR2
      HCT=.45*HCT/(R*R)
```

```
C   CALCULATE DISSIPATED ENERGY
C
C
      ENDIS(I2)=PFLUX*M*DT+HCT-HCO
C
C   CHECK IF DEPOSIT IS ENTIRELY FROZEN
C
      IF(ENDIS(I2).GE.ENMAX)GOTO 11
      IF(TF.GE.TIM)GOTO 6
1     CONTINUE
11    CONTINUE
      IF((ENDIS(I2)-ENMAX).GE.(ENMAX-ENDIS(I1)))
     *I2=I1
6     CONTINUE
      TF=TF-.5*DT
      OFLUX=PFLUX*TF
      L=IR+1
      DO 7 I=1,L
      IF(I2.EQ.2)U(I,1)=U(I,2)
      U(I,5)=U(I,5)/M
7     U(I,3)=U(I,I2)
      WRITE(6,100)TF,DT,ENMAX,ENDIS(I2),OFLUX,HCO,
     *HCT
100   FORMAT(1H0,5E12.5,2D20.5)
      RETURN
150   IR=1
      RETURN1
      END
```

```
C   THIS SUBROUTINE SOLVES THE HEAT EQUATION WITH THE
C   SECOND BOUNDARY CONDITION.
C   THE CRANK-NICHOLSON METHOD IS USED.
C
C
      SUBROUTINE COOL (IP,IT,TC,TIM,C12,T,P,R,I1,
     *I2)
      COMMON/BLOCK1/U(101,6)
      DIMENSION CSTAR(100),DSTAR(100),TT(50)
      DOUBLE PRECISION U,CSTAR,DSTAR,ALM,GAM,HCF,
     *DR2,D1
      DT=TC/IT
      IHALF=IT/2
      DR=R/IR
      ALM=.0109*DT/(DR*DR)
      BETA=ALM/(ALM+2.)
      ALM=ALM*(1.-1./(ALM+2.))
      GAM=-ALM*2.-1.
      VFLUX=0.
      MLIM=IT
      CSTAR(1)=ALM/GAM
      Q1=3.39E-02*((T*P/R)**.25)
      Q2=660.*C12*(T**.1)/((P**.75)*(R**.25))
      ESV=VAP(T)
C
C
C   START TIME ITERATIONS
C
      DO 1 M=1,MLIM
      I2=MOD(M,2)+1
      I1=I2-1
      IF(I1.EQ.0)I1=2
C
C
C   CALCULATE THE TRANSFORMED COEFFICIENTS BY THE
C   THOMAS ALGORITHM
C
      DSTAR(1)=-(U(2,I1)*(1.-2.*BETA)+BETA*U(3,I1)
     *)/GAM
      II=IR-2
      DO 2 I=2,II
      CSTAR(I)=ALM/(GAM-ALM*CSTAR(I-1))
      DI=-(U(I+1,I1)*(1.-2.*BETA)+BETA*(U(I,I1)+
     *U(I+2,I1)))
2     DSTAR(I)=(DI-ALM*DSTAR(I-1))/(GAM-ALM*
     *CSTAR(I-1))
```

```
C   CALCULATE VALUES AT THE TWO INNER SURFACE
C   POINTS BY THE METHOD OF FALSE POSITION
C
C
      DI=-(U(IR,I1)*(1.-2.*BETA)+BETA*(U(IR-1,I1)
     *+U(IR+1,I1)))
      A=((DI-ALM*DSTAR(II))/(GAM-ALM*CSTAR(II))
     *-DSTAR(II)/(4.+CSTAR(II)))/R
      B=(3.-2.*DR/R)/(4.+CSTAR(II))+ALM/(GAM-ALM*
     *CSTAR(II))
      FXO=DR*(Q1*(273.-T)+Q2*(6.107-ESV))*2./(4.+
     *CSTAR(II))-A
      XN=T-273.
      DO 3 L=1,20
      ESVI=6.109177956+XN*(5.03469897E-01+XN*
     *(1.886013408E-02+XN*(4.176223716E-04+XN*
     *(5.82472028E-06+XN*(4.838803174E-08+
     *XN*1.838826904E-10)))))
      FXN=B*XN+DR*(Q1*(XN+273.-T)+Q2*(ESVI-ESV))
     **2./(4.+CSTAR(II))-A
      XN1=-XN*FXO/(FXN-FXO)
      AV=XN1-XN
      IF(AV.LE..001)GOTO 4
      XN=XN1
3     CONTINUE
4     U(IR+1,I2)=XN1*R
      ESVI=6.109177956+XN1*(5.03469897E-01+XN1*
     *(1.886013408E-02+XN1*(4.176223716E-04+XN1*
     *(5.82472028E-06+XN1*(4.838803174E-08+
     *XN1*1.838826904E-10)))))
      QV=Q1*(XN1+273.-T)+Q2*(ESVI-ESV)
      U(IR,I2)=(DI-ALM*(U(IR+1,I2)+DSTAR(II)))/
     *(GAM-ALM*CSTAR(II))
      VFLUX=VFLUX+.005*QV*DT
      U(IR+1,6)=U(IR+1,6)+U(IR+1,I2)
      U(IR,6)=U(IR,6)+U(IR,I2)
      II=IR-1
C
C
C   CALCULATE VALUES AT INTERIOR POINTS
C
      DO 5 N=2,II
      U(IR+1-N,I2)=DSTAR(IR-N)-CSTAR(IR-N)*
     *U(IR+2-N,I2)
5     U(IR+1-N,6)=U(IR+1-N,6)+U(IR+1-N,I2)
      TT(M)=XN1
      IF(M.NE.IHALF)GOTO 1
```

```
C   STORE VALUES AT THE TENTH TIME STEP
C
      IN=IR+1
      DO 66 N=1,IN
66    U(N,4)=U(N,I2)
1     CONTINUE
C
      DO 99 N=1,IN
99    U(N,6)=U(N,6)/IT
C
C   CALCULATE FINAL HEAT CONTENT
C
      DR2=DR*DR
      HCF=0.
      DO 77 N=2,IR
77    HCF=HCF+(N-1)*U(N,I2)
      HCF=(HCF+(IR)*U(IR+1,I2)/2.)*DR2
      HCF=HCF*.45/(R*R)
      WRITE(6,100)TC,VFLUX,HCF,AV
      WRITE(7,200)(TT(I),I=1,IT)
      TB=0.
      TB2=0.
      DO 88 I=1,IT
      TB=TB+TT(I)
88    TB2=TB2+TT(I)*TT(I)
      TB=TC/TIM*TB/IT
      TB2=SQRT(TC/TIM*TB2/IT-TB*TB)
      WRITE(7,200)TB,TB2
200   FORMAT(5X,15F8.2)
100   FORMAT(1H0,2F10.5,D20.5,F30.10)
      RETURN
      END
```

APPENDIX 2

## LISTOGRAM

The Listogram gives solutions of equation (1.2) - actually, this equation divided by $v^{\frac{1}{2}}$ - in graphical form. For a given air temperature and liquid water content, the hailstone temperature and ice fraction are found or interpolated from the labeled curves on the graph. The air temperature, pressure and height are related according to a simple cloud model given in List et al. (1965). Therefore one must be careful to select the appropriate temperature and pressure in order to calculate the Reynold number Re, (equation (2.13)). However, List et al. (1967) claim that

$$\phi = Ew_f\theta^{-1} Re^{-\frac{1}{2}} = 55.84\, D^{.75}$$

with an accuracy of better than ± 13 percent. The product $w_f\phi$ allows to get an easy estimate of the hailstone temperature from the diagram.

The heavy continuous lines on the Listogram define the regions where one heat transfer is dominant. The ratios are defined as follows:

$$R_{CC/F} = \frac{Q_{CP}}{Q_F}$$

$$R_{E/F} = \frac{Q_{ES}}{Q_F}$$

$$R_{CP/F} = \frac{Q_{CP}}{Q_F}$$

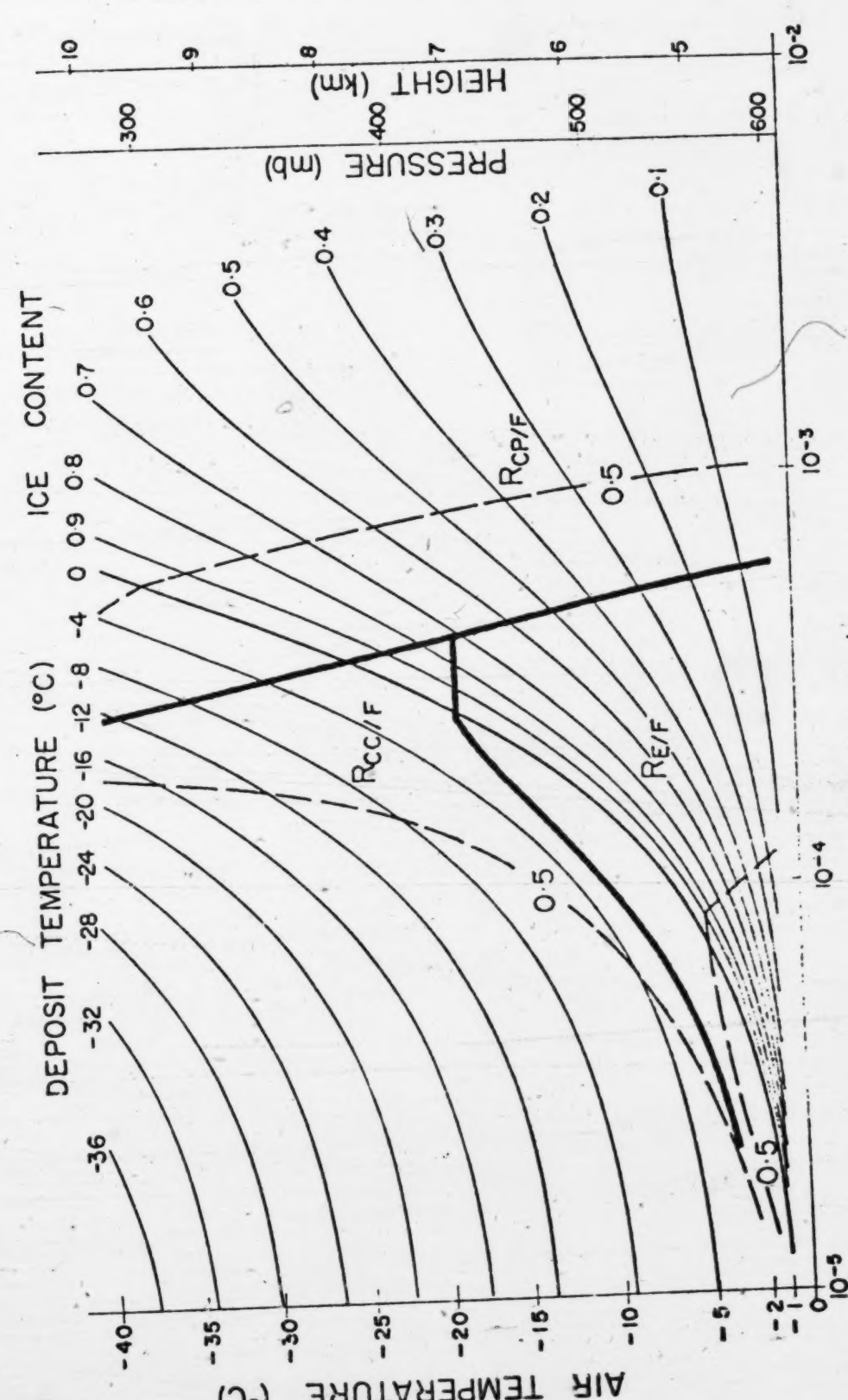


Figure A-1. Listogram

The dashed lines define regions where those transfers are absolutely dominant, that is, greater than .5.